J. Neural Eng. **8** (2011) 046025 (20pp) doi:10.1088/1741-2560/8/4/046025

# True associations between resting fMRI time series based on innovations

**P Christova[1,2], S M Lewis[1,3], T A Jerde[1,2,4], J K Lynch[1,2] and A P Georgopoulos[1,2,3,5,6,7]**

[1] Brain Sciences Center, Veterans Affairs Health Care System (11B), Minneapolis, MN 55417, USA
[2] Department of Neuroscience, University of Minnesota Medical School, Minneapolis, MN 55455, USA
[3] Department of Neurology, University of Minnesota Medical School, Minneapolis, MN 55455, USA
[4] Current address: Department of Psychology, New York University, New York, NY 10003, USA
[5] Department of Psychiatry, University of Minnesota Medical School, Minneapolis, MN 55455, USA
[6] Center for Cognitive Sciences, University of Minnesota, Minneapolis, MN 55455, USA

E-mail: omega@umn.edu

Received 21 December 2010
Accepted for publication 3 June 2011
Published 29 June 2011
Online at stacks.iop.org/JNE/8/046025

**Abstract**

We calculated voxel-by-voxel pairwise crosscorrelations between prewhitened resting-state BOLD fMRI time series recorded from 60 cortical areas (30 per hemisphere) in 18 human subjects (nine women and nine men). Altogether, more than a billion-and-a-quarter pairs of BOLD time series were analyzed. For each pair, a crosscorrelogram was computed by calculating 21 crosscorrelations, namely at zero lag ± 10 lags of 2 s duration each. For each crosscorrelogram, in turn, the crosscorrelation with the highest absolute value was found and its sign, value, and lag were retained for further analysis. In addition, the crosscorrelations at zero lag (irrespective of the location of the peak) were also analyzed as a special case. Based on known varying density of anatomical connectivity, we distinguished four general brain groups for which we derived summary statistics of crosscorrelations between voxels within an area (group I), between voxels of paired homotopic areas across the two hemispheres (group II), between voxels of an area and all other voxels in the same (ipsilateral) hemisphere (group III), and voxels of an area and all voxels in the opposite (contralateral) hemisphere (except those in the homotopic area) (group IV). We found the following. (a) Most of the crosscorrelogram peaks occurred at zero lag, followed by ±1 lag; (b) over all groups, positive crosscorrelations were much more frequent than negative ones; (c) average crosscorrelation was highest for group I, and decreased progressively for groups II–IV; (d) the ratio of positive over negative crosscorrelations was highest for group I and progressively smaller for groups II–IV; (e) the highest proportion of positive crosscorrelations (with respect to all positive ones) was observed at zero lag; and (f) the highest proportion of negative crosscorrelations (with respect to all negative ones) was observed at lag = 2. These findings reveal a systematic pattern of crosscorrelations with respect to their sign, magnitude, lag and brain group, as defined above. Given that these groups were defined along a qualitative gradient of known overall anatomical connectivity, our results suggest that functional interactions between two voxels may simply reflect the density of such anatomical connectivity between the areas to which the voxels belong.

[7] Author to whom any correspondence should be addressed.

 

## 1. Introduction

During the past 15 odd years, an increasing number of studies have been carried out on time series of functional brain neuroimaging data, especially obtained using functional magnetic resonance imaging (fMRI). In 1995, Biswal *et al* [1] were the first to report significant correlations between fMRI time courses (filtered <0.1 Hz) obtained for different voxels in the motor cortex, in the absence of a task (resting) and during bilateral finger tapping. Similar studies of correlating fMRI time courses in the resting state in various brain areas became more and more frequent during the subsequent years; these studies are summarized in two recent reviews [2, 3] and will not be discussed here. The common methodological feature of those studies is the correlation of raw time courses, commonly subjected to some pre-processing, including spatial smoothing, corrections for global fluctuations, etc (see, for example, [2, 4–6]). Unfortunately, no attention has been paid to the fundamental problem inherent in correlating any pair of time series, namely the nonstationarity and autocorrelation of the individual series being correlated. The problem is that, unless these issues are taken explicitly into account, correlations between such time series are most likely to be spurious, since they will reflect both the internal properties of the series as well as any 'true' relation between the two series. In addition, it is likely that the regression errors (residuals) will be typically serially correlated, in violation of a fundamental assumption in least-squares regression analysis, namely that regression errors be independent, i.e. not serially correlated [7, 8]. Such a violation invalidates least-squares regression and is guaranteed to yield spurious correlations [7]. These pitfalls were first noted several decades ago [7, 10–18] in statistics [7, 9, 10, 13, 15, 17, 18]. A famous case in econometrics was a paper with spurious results [11], refuted shortly thereafter [12] using prewhitening techniques. The recognition of the serious errors stemming from autocorrelated regression errors and the application of proper analyses in econometrics were pioneered by Box, Newbold, Granger and others [12, 14, 16]; the problem was also recognized, more recently, in neurophysiology [19]. Remarkably, the serious problem of spurious correlations derived from correlating nonstationary time series was specifically cited by the Nobel Prize committee in awarding the Nobel Prize in Economic Sciences to Clive W J Granger in 2003 [20] and was discussed by Granger himself in his Nobel Prize lecture [21]. The remedy, pioneered by Box, Priestley, Newbold, Granger and others [7, 9, 12–18, 22–25], is to first render the individual, univariate time series, e.g. $X_t$ and $Y_t$, stationary and nonautocorrelated by suitably modeling the series and taking the stationary and nonautocorrelated residuals (also called 'innovations'), $R(X)$ and $R(Y)$: the correlation between these residuals is the true correlation between the two time series (see [15] for a lucid exposition). This preprocessing is called 'prewhitening' of the series and is typically accomplished by fitting an AutoRegressive Integrative Moving Average (ARIMA) model [10, 25]. Without prewhitening, the correlations between raw time series are very likely to be spurious, and, at least, do not reflect the true association between the two series (see [16], pp 202–14 and pp 230–7, for a particularly lucid discussion of this issue). In previous studies, since 1995, we applied this method to fMRI data to detect task effects [26, 27] (see also [28]) and perform brain network analyses during cognitive processing [29–31]. In addition, we used this method of correlating prewhitened neural time series on magnetoencephalographic (MEG) data to investigate task differences [32] and assess the potential for such correlations to discriminate among, and classify, brain diseases in the resting state [33–36]. In this study, we applied this method on resting fMRI (rfMRI) data to assess true associations between voxels within a specific region of interest (ROI), between voxels of a given ROI and voxels of the same ROI in the opposite hemisphere (homotopic ROI), between voxels of a given ROI and other voxels in the same hemisphere, and between voxels of a given ROI and other voxels in the opposite hemisphere (excluding those in the homotopic ROI). We found systematic effects on the strength and sign of correlations among those four groups which reveal a basic pattern of associations in a task-free state.

## 2. Materials and methods

### 2.1. Subjects

Eighteen healthy human subjects participated in these experiments as paid volunteers. They ranged in age from 21 to 44 years; nine were men (32.9 ± 2.2 years, mean ± SEM; range: 25–44 years) and nine were women (25.2 ± 1.1 years; range 21–32 years). All subjects participated in the study after providing informed consent, in adherence to the Declaration of Helsinki. The study protocol was approved by the respective Institutional Review Boards.

### 2.2. Task

The experimental task was simple, short, did not require a practice session and engaged the brain in a stable condition. Subjects lay supine within the scanner and fixated their eyes on a spot in front of them in the center of the screen. The absence of eye movement during this fixation period was verified by using an eye tracking system (ASL eye tracker, Applied Science Laboratories, Bedford, MA). Subjects were asked to remain still. Participants wore earplugs to reduce the scanner noise.

### 2.3. Image acquisition

Blood oxygenation level dependent (BOLD) contrast functional images were acquired with a whole-body 3 T MRI scanner (Magnetom Trio, Siemens, Erlangen, Germany) at the Center for Magnetic Resonance Research of the University of Minnesota using a gradient echo echo-planar imaging (EPI) ($T2^*$) sequence with the following parameters: echo time (TE) = 23 ms; repetition time (TR) = 2 s; flip angle = 90°; in-plane resolution, 3 mm × 3 mm; slice thickness, 3 mm without inter slice gap. Whole-brain functional volumes ($N$ = 203) of 38 axial slices covering the whole brain, cerebellum,

and brain stem were obtained for each subject. A high-resolution anatomical T1-weighted 3D flash scan was obtained with the following parameters: TE = 4.7 ms; TR = 20 ms; flip angle = 22°; in-plane resolution = 1 mm × 1 mm; slice thickness = 1 mm; 176 slices in total.

### *2.4. Data extraction*

All analyses were performed on the BOLD time series signal acquired per individual voxel in the whole brain of each subject. Coordinates in Talairach space for each voxel, as well as the BOLD intensity for each voxel, were extracted using Brain Voyager QX (v.1.10, Brain Innovation BV, Maastricht, The Netherlands). Slice scan time correction was performed using *sinc* interpolation based on the information about TR and interleaved order of slice scanning. Three-dimensional motion correction was performed to correct for small head movements, if present, by spatially aligning all volumes of a subject to the first volume using rigid body transformations. The estimated parameters of translation and rotation were inspected and did not exceed 3 mm or 2°. The 3D volumes were then aligned with the corresponding 3D anatomical volumes and normalized to standard Talairach space [37]. Matlab (R2008b, Mathworks, Natick, MA, USA) programs were implemented to enable BOLD time series extraction from volume time course and anatomical mask available from Brain Voyager. For each subject, 203 functional images were acquired continuously, yielding a sequence of 203 BOLD signal values per voxel; of these, the first three volumes were discarded, leaving a time series of 200 BOLD values for analysis. Because the coefficient of variation is higher in the vicinity of large vessels and outside the brain [38], we analyzed only voxels with coefficient of variation of no more than 5%.

A high-speed database server called Talairach Daemon [39, 40] was used for automatic brain segmentation of individual brains in Talairach space. Talairach coordinates of each voxel were used to search the Talairach Daemon database (www.talairach.org, v.2.4.2) for the Talairach label using the 'single point' search option. All voxels of the gray matter of the following 30 areas of the cerebral cortex in the left and right hemispheres were analyzed (for a total of 60 areas): precentral gyrus, superior frontal gyrus, middle frontal gyrus, inferior frontal gyrus, precentral lobule, medial frontal gyrus, rectal gyrus, subcallosal gyrus, orbital gyrus, postcentral gyrus, superior parietal lobule, inferior parietal lobule, angular gyrus, supramarginal gyrus, precuneus, superior occipital gyrus, middle occipital gyrus, inferior occipital gyrus, cuneus, lingual gyrus, superior temporal gyrus, middle temporal gyrus, inferior temporal gyrus, transverse temporal gyrus, fusiform gyrus, cingulate gyrus, anterior cingulate, posterior cingulate, parahippocampal gyrus, uncus.

### *2.5. Data preprocessing: prewhitening the raw BOLD time series*

Initial inspection of the BOLD time series from many voxels revealed that they were nonstationary with respect to the mean and highly autocorrelated. (The variance did not vary much along the series.) Since we were interested in calculating the crosscorrelation function (CCF) between these time series, it is required, from first principles [10, 13–15, 17], that individual series be rendered stationary and nonautocorrelated for their crosscorrelation to be valid (i.e. not spurious). 'Stationarity' implies that statistical parameters do not vary along the time series, i.e. they are more or less constant at different time points $t$, i.e. for small time intervals centered at $t$. There are three parameters of interest: mean, variance and autocovariance. A simple plot of the data and a plot of the autocorrelation function would typically go a long way to begin assessment of the time series and decide on initial steps to render it stationary. For example, inspection of the raw BOLD time series plots for the two voxels in the top panel of figure 1 shows that BOLD values vary with time (indicating the presence of time trends, i.e. that the series is 'integrated' [14, 16]); moreover, inspection of the corresponding autocorrelation plots of these series in figure 2 (top panel) shows a strong dependence of BOLD values on previous values, up to 15 lags being plotted. On the other hand, the variance of BOLD values does not seem to vary systematically with the time-varying mean. This initial qualitative assessment suggests that the series is nonstationary and autocorrelated. The objective now is to render the series stationary and nonautocorrelated, i.e. convert it to white noise, hence the term 'prewhitening'. The strategy [7, 10, 15, 17, 22, 25] is to model the series and then apply the model and take the residuals; the better the modeling of the series is, the closer the residuals will be to white noise. This prewhitening is commonly achieved in two stages. The first stage is called *model identification* and consists in identifying the factors that are relevant for the internal structure of the series. The tools for this step consist of inspecting the series and plotting autocorrelation functions, including the raw autocorrelation (ACF, i.e. the correlation between $X_t$ and $X_{t-k}$) and the partial autocorrelation (PACF, i.e. the correlation between $X_t$ and $X_{t-k}$ when all intervening relations between $X_t$ and $X_{t-k}$, namely between $X_t$ and $\{X_{t-1}, \ldots, X_{t-k-1}\}$ have been accounted for, that is 'partialed out'). Based on the data time series plot and the shape of ACF and PACF, a tentative model is suggested with respect to three kinds of basic factors: dependence of a value on previous values ('AutoRegressive, AR' component of the model), presence of time trends ('Integrative, I' component of the model), and dependence of a value on the variation of previous values ('Moving Average, MA' component). Following the pioneering work of Box and Jenkins [10], this is called ARIMA modeling of a time series (from the capitalized initials of the three model components above). An ARIMA model is concisely described as of ($p$, $d$, $q$) orders, where $p$ denotes the AR orders (i.e. the number of AR lags in the model), $d$ denotes the I orders (i.e. the number of differencing in the model), and $q$ denotes the MA orders (i.e. the number of MA lags in the model). After a tentative choice of ($p$, $d$, $q$) orders, we proceed in the second stage, namely *model parameter estimation.* This stage involves computations which are commonly implemented in several statistical packages and which yield coefficients for the AR and MA lags specified. Typical diagnostic checking of the model involves plotting the residuals, their ACF and PACF, ensuring that the AR and MA

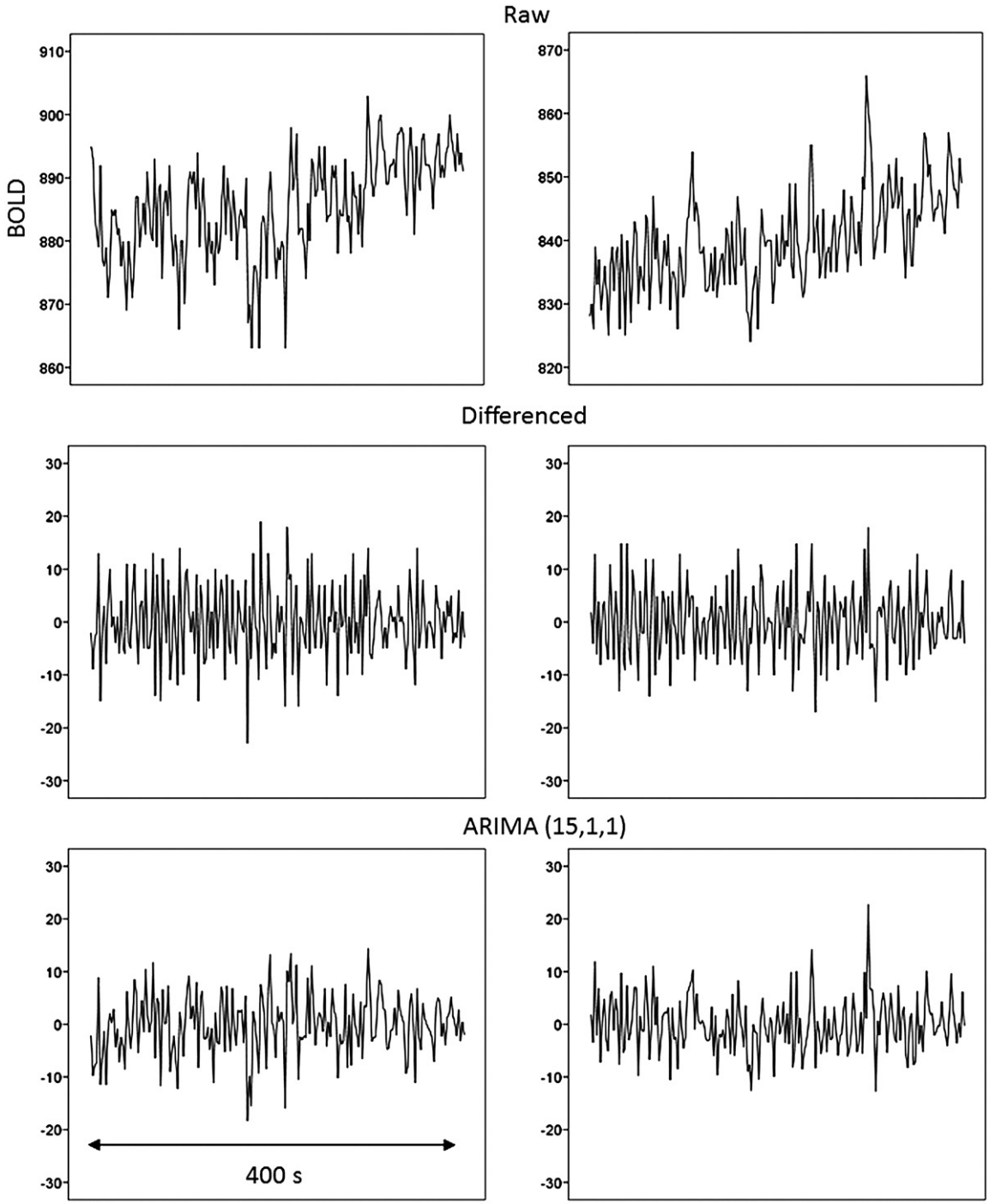


**Figure 1.** Resting fMRI time series recorded from 2 voxels in the left superior parietal lobule of a single subject after various stages of processing, as indicated.

coefficients are within bounds of stationarity and invertibility, respectively, and calculating some global measures, including the sums of the squares of residuals, Akaike's information criterion, Schwartz's Bayesian criterion, etc. The essential point for our application is not really to model the series perfectly (this could be an *ad hoc* objective of another study aimed to elucidate the various dependences in a BOLD time series) but to model it adequately enough so that the residuals obtained are stationary and nonautocorrelated. If indeed so, we retain them for the subsequent crosscorrelation analysis; otherwise, the model is further refined iteratively by varying the $(p, d, q)$ orders until this goal is attained.

Typically, we start with ($p = 0$, $d = 1$, $q = 0$) which involves first-order differencing: $X_t - X_{t-1}$ (see below). This aims to remove nonperiodic time trends which are ubiquitous, even in random walks [14, 16]. (For a particularly instructive explication of this problem, see [14] and [16], pp 202–14 and pp 230–7.) (Periodic trends, if present, say at lag $k$ are removed by differencing at that lag: $X_t - X_{t-k}$.) It can be seen in figure 1 (middle panel) that this process indeed removed

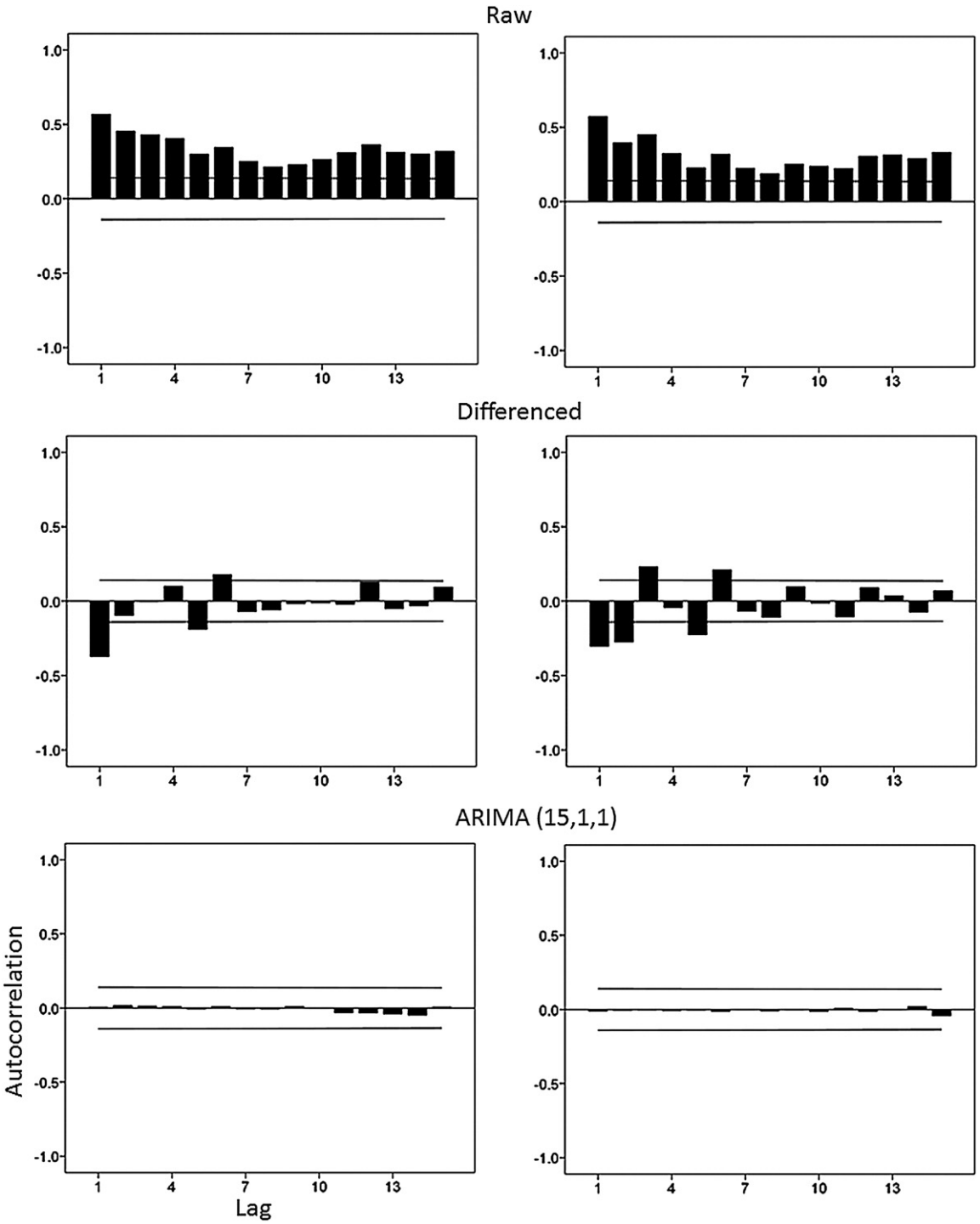


**Figure 2.** Autocorrelation functions of the time series in figure 1 after various stages of processing. Notice that the innovations series (i.e. residuals) after ARIMA (15, 1, 1) are nonautocorrelated. Lines on either side of the abscissa indicate 5% statistical significance levels.

the trends and that now the mean of the series is centered near zero. However, differencing was not adequate: the ACF plots of the differenced series (figure 2, middle panel) show a big improvement in reducing autocorrelations as compared to the raw data (figure 2, top panel) but the ACF of the ($p = 0$, $d = 1$, $q = 0$) residuals contain a number of statistically significant autocorrelations, especially at the first few lags which are the most important for our application. (That simple differencing was in general insufficient is indicated by the plots in figure 3.) This outcome indicates that further modeling is required. Indeed, extensive iterative investigation yielded an ARIMA model of ($p = 15$, $d = 1$, $q = 1$), or (15, 1, 1) for short, which yielded stationary (figure 1, bottom panel) and nonautocorrelated (figure 2, bottom panel) residuals. Following Priestley [18], we call these residual series 'innovations', to denote the '*essentially "new" part of* $X_{t+1}$, in the sense that it represents that part of $X_{t+1}$ which is not linearly dependent on past observations' ([18], p 740, italics

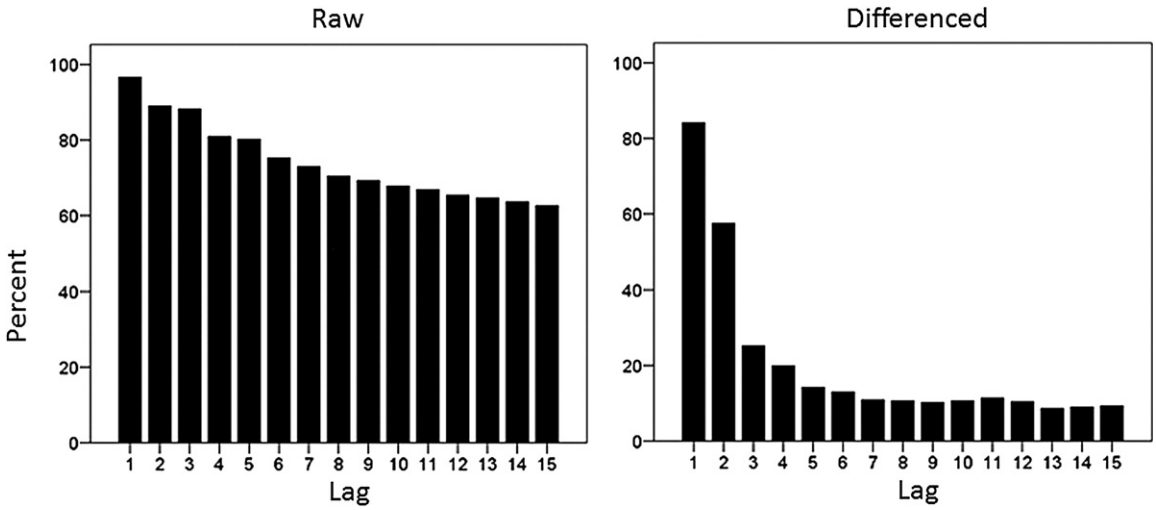


**Figure 3.** Percentages of autocorrelations in raw and differenced resting fMRI time series exceeding a ∼95% confidence interval as threshold are plotted against the absolute lag (see the text). Notice (a) the very high percentage of autocorrelations exceeding threshold, and (b) that differencing is not sufficient to yield nonautocorrelated residuals, hence the need for additional (ARMA) components in the time series model.

in the original). (Priestley also provides a nice geometrical interpretation of the innovations process in [18], figure 10.3, p 740.) We used the SPSS statistical package for Windows (version 15, SPSS Inc., Chicago, IL, 2006) to carry out the ARIMA modeling. Our choice of 15 AR lags was dictated by the fact that our crosscorrelation analysis extended up to 10 lags, so we wanted to ensure lack of autocorrelation for a few lags beyond 10.

### 2.6. ARIMA equations

The formal ARIMA equations are given in practically every textbook on time series (see [25] for the most recent textbook by Box *et al*). However, we give them here too for the purpose of clarity. We present below the standard equations. (In time series analysis, use is made frequently of the backshift and del notation which can be found in time series textbooks.)

*2.6.1. Integrative (I) model.* Time series are often nonstationary, i.e. typically show an average increase or a decrease in their value over time (see, e.g., the raw BOLD time series in figure 1, top panels). As mentioned in the preceding paragraph, the first step is to make the series stationary in its mean. This is achieved by differencing. Consider a BOLD series $X(t)$ with TR = 2 s, where there is an upward linear trend (e.g., top-right plot in figure 1). This means that every 2 s the series increases on average (in expectation) by some constant amount $C$. Since

$$X_t = C + X_{t-1} + N_t \tag{1}$$

where $N_t$ is a random 'noise' component with expectation zero,

$$X_t - X_{t-1} = C + N_t. \tag{2}$$

Thus $N_t + C$, or just $N_t$, is a stationary process with the linear trend removed. Let $z_t$ be the stationary series obtained by differencing series $X_t$:

$$z_t = X_t - X_{t-1}. \tag{3}$$

*2.6.2. AutoRegressive (AR) model.* The AR model refers to dependence on past values of the series. Obviously, it can only be applied to a stationary series, i.e. to a series without trend (otherwise, the estimated dependence on previous values would include the trend, and hence would be spurious and invalid). Given the stationary series $z_t$, the AR model implies a linear dependence of $z_t$ on previous values $\{z_{t-1}, z_{t-2}, \ldots, z_{t-k}\}$, and is similar to a linear regression model. The highest lag $k$ specifies the order $p$ of the AR model. At any time

$$z_t = C + \Phi_1 z_{t-1} + \Phi_2 z_{t-2} + \cdots + \Phi_\kappa z_{t-k} + a_t, \tag{4}$$

where $C$ is the constant level, $\{z_{t-1}, z_{t-2}, \ldots, z_{t-k}\}$ are past series values (lags), the $\Phi$s are coefficients (similar to regression coefficients) to be estimated, and $a_t$ is a random variable with mean zero and constant variance. The $a_t$s are assumed to be independent and represent random errors or random shocks.

*2.6.3. Moving Average (MA) model.* The MA model refers to the dependence on the past values of the random shocks above. (Again, this can only be applied to a suitably differenced, stationary series.) Given the stationary series $z_t$, the MA model implies a linear dependence of $z_t$ on previous values $\{a_{t-1}, a_{t-2}, \ldots, a_{t-m}\}$. The highest lag $m$ specifies the order $q$ of the MA model. At any time,

$$z_t = a_t - \Theta_1 \alpha_{t-1} - \Theta_2 \alpha_{t-2} - \cdots - \Theta_\kappa \alpha_{t-m}. \tag{5}$$

This model is called moving average because $z_t$ is assumed to be a weighted average of the uncorrelated $a_t$s.

*2.6.4. Combined ARMA model.* The AR and MA models can be combined to an ARMA model of the stationary series $z_t$ to account for both past values and past random shocks. Note that, similar to the AR and MA cases, the ARMA model can *only* be applied to a suitably differenced stationary process; it is incorrect and invalid to apply such a model to series with

trends. Consider an ARMA model with ($p = 3$, $q = 2$) of the stationary series $z_t$. The combined model is then

$$z_t = C + \Phi_1 z_{t-1} + \Phi_2 z_{t-2} + \Phi_3 z_{t-3} + a_t - \Theta_1 \alpha_{t-1} - \Theta_2 \alpha_{t-2}. \quad (6)$$

Given that $z_t$ is a stationary, once-differenced series, the complete model for the original series $X_t$ is an ARIMA model with ($p = 3$, $d$ =1, $q = 2$).

### 2.7. Crosscorrelations

Crosscorrelations $r$ between the innovations series of each pair of voxels were calculated for 10 lags, corresponding to 20 s, given TR = 2 s. (It should be noted that these crosscorrelation lags are unrelated to the autocorrelation lags used for ARIMA modeling and diagnostics.) In addition to the lag-based analysis, we also analyzed the zero-lag crosscorrelations as a special case.

### 2.8. Data transformations

For statistical analyses, standard transformations were applied to specific data as follows to stabilize their variance and normalize their distributions [41].

(a) Correlations were $z$-transformed [42]: $z = 0.5[\log_e(1+r) - \log_e(1-r)]$.
(b) Ratios were log-transformed: ratio$' = \log_e$(ratio).
(c) Proportions were arcsin-transformed: proportion$' =$ arcsin(proportion); for plotting purposes, proportions were converted to percentages.

The double-precision functions of the IMSL statistical library in FORTRAN were used for all computations using personal computers (Compaq Visual Fortran Professional Edition, version 6.6B) and a 512-core Linux cluster (Rocks 5.1, CentOS 5.2, Intel Fortran Compiler 10.0, IMSL 6.0).

### 2.9. Statistical analyses

Standard statistical analyses were performed [41], including analysis of covariance (ANCOVA), linear regression, $t$-test, etc. The SPSS statistical package for Windows (version 15) was used for this purpose. The Durbin–Watson test (and its statistical significance for testing the null hypothesis that serial correlation of regression residuals is zero) was computed using Matlab R2010b, version 7.11.0.584 (64 bit).

### 2.10. Brain groups

Crosscorrelations were calculated for each pair of voxels. These voxel pairs were assigned as follows to one of four groups. In the *intra-area* group (group I), both voxels in a pair were located within the same area; in the *homotopic* group (group II), one voxel was located in a given area and the other in the same area of the opposite hemisphere; in the *ipsi-hemispheric* group (group III), one voxel was located in a given area and the other in any other area of the same hemisphere; finally, in the *contra-hemispheric* group (group IV), one voxel was located in a given area of one hemisphere and the other in any nonhomotopic area of the opposite hemisphere. Various statistics (e.g. means) were calculated for each group across subjects.

## 3. Results

### 3.1. General

Data (i.e. BOLD time series) were available from 212 227 voxels in the 60 brain areas above (30 areas for each hemisphere) corresponding to 1 255 517 520 pairs. Given that we computed a crosscorrelogram with 21 values (0 ± 10 lags) for each pair, the total number of crosscorrelations calculated was 26 365 867 920.

### 3.2. ARIMA

The raw BOLD times series were typically nonstationary and highly autocorrelated (figures 1 and 2, top panel). Following differencing, the series became centered on zero (figure 1, middle panel) but significant autocorrelations remained (figure 2, middle panel). These were removed after applying the full ARIMA (15, 1, 1) model (see section 2) which yielded innovations series (i.e. residuals) centered on zero with lower variance (figure 1, bottom panel) and nonautocorrelated values (figure 2, bottom panel).

These changes in autocorrelations were quantified by calculating the percentage of autocorrelations that exceeded an arbitrary threshold, namely that the absolute value of an autocorrelation at a specific lag was higher than twice its standard error. (This threshold corresponds approximately to a 5% probability level for a single autocorrelogram.) Figure 3 shows these percentages for different lags for the raw and differenced (i.e. detrended) data. It can be seen that very high percentages of autocorrelations exceeded threshold for the raw data, and that high percentages remained for the first two lags in the detrended (differenced) data. This latter finding indicates that autocorrelations exceeding threshold are not just due to time trends but are inherent to the BOLD time series. In contrast, the percentages for the ARIMA (15, 1, 1) innovations process exceeding threshold were extremely small and are not shown (for that reason). Specifically, the mean percentage (±SEM, $N = 15$ lags) of autocorrelations exceeding threshold in the ARIMA innovations series was 0.0159% ± 0.008 24, as compared to 74.3% ± 2.72 for the raw series and 20.34% ± 5.57 for the differenced (detrended) series.

### 3.3. Crosscorrelations

As expected from the presence of trends and high autocorrelations above, crosscorrelations between raw BOLD time series were very inflated (figure 4, upper panel), as compared to the crosscorrelations between the ARIMA innovations series (figure 4, lower panel). In fact, differences need not be restricted to the magnitude of the correlation but they affect its sign and lag, as illustrated in additional examples in figure 5 (see also [16] pp 230–7). The correlations between raw time series are spurious, and those between the ARIMA innovations series are correct.

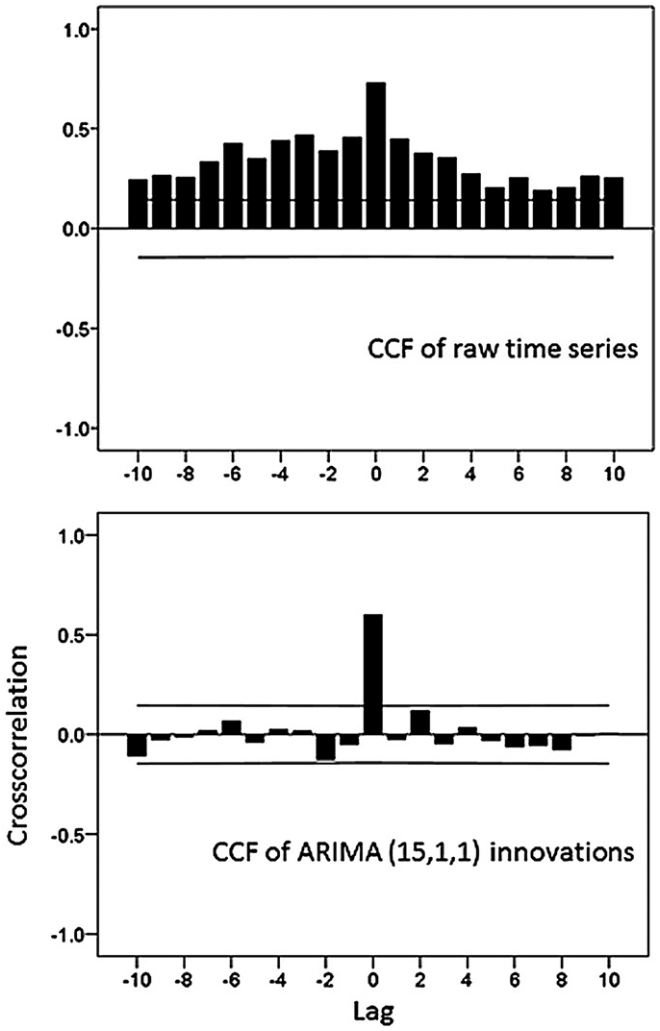


**Figure 4.** CCFs between the series illustrated in figure 1 for the raw and ARIMA innovations. Notice the spurious, widespread high crosscorrelations in the raw data, as contrasted with the true, single high zero-lag crosscorrelation of the innovation series.

*3.3.1. Serial correlations in regression residuals.* The spuriousness of the correlations between raw time series (top panel of figure 4 and left panel of figure 5) stems not only from first principles [10, 12–18], recognized in Granger's Nobel Prize Citation [21] and his Nobel Prize Lecture [20], but also from the fact that correlating nonstationary time series typically violates a fundamental assumption of least-squares regression, namely that regression errors (i.e. residuals) be independent [7, 8, 41]; if regression errors are serially correlated, the correlation coefficient calculated is spurious. The estimates of *any* least-squares regression analysis with serially correlated errors are invalid, with typically low estimates of standard errors and hence inflated statistical significance of the slope and inflated correlation coefficient. These detrimental effects of serially correlated errors are being explicated in practically every standard textbook of elementary (or sophisticated) statistics, for the problem is specific to regression/correlation of any data, not just time series. For example, a standard textbook on regression [8] devoted 16 pages (pp 153–69) to just this issue. Fortunately, there is a special test by which to detect serial correlation in regression residuals, namely the Durbin–Watson test [43, 44], developed 60 years ago. The Durbin–Watson test can tell us whether a violation of error independence exists, and whether it is significant. Therefore, this is an objective measure by which to test the validity of any analysis, including any such analysis of neural associations reported in this paper as well as in the literature. Since we do not have access to data published in the literature from other groups, we carried out an extensive analysis of the residuals in a sample of 300 voxels (yielding 44 850 pairwise correlations) from our data, under three conditions: (a) raw time series, (b) time series filtered as described by Fox *et al* [4] ($0.009 < f < 0.08$ Hz), and (c) prewhitened time series, as described above. For each pair, we calculated the autocorrelation function of the residuals and the corresponding Durbin–Watson test statistic $d$. We illustrate the results in figures 6 and 7. In figure 6 (left panel), we plot three CCFs for a pair of voxels. It can be seen that they are drastically different, and that the crosscorrelations of the raw and filtered time series are very inflated. In fact, both the high values of the correlations and the smooth shape of the crosscorrelograms of nonstationary series make them suspect, as succinctly discussed by Granger and Newbold: 'Thus, not only does one have to contend with the spurious regression phenomenon of the size of the cross correlations, but also the *shape* of the cross correlogram is impossible to interpret sensibly' ([16], p 232). In the right panel of figure 6, we plot the autocorrelation functions of the residuals for the zero-lag crosscorrelation: it can be seen that the residuals are highly autocorrelated for both the raw and filtered data, with lag 1 serial correlation close to 0.8. The Durbin–Watson statistic $d$ was 1.237 for the raw data regression, 0.281 for the filtered data and 2.095 for the prewhitened data (the smaller the value of $d$, the higher the serial correlation of the residual, the more suspect the correlation coefficient [16]). The critical value ($p < 0.05$) of $d$ in our sample is 1.753: any value below it rejects the null hypothesis that the serial correlation of the residuals is zero, so only the prewhitened data yield correct estimates. The spuriousness of high correlations associated with low $d$ is beautifully discussed and illustrated in [14, 16] (see also [21, 20]). Finally, in figure 7, we plot histograms of all Durbin–Watson $d$ values obtained in this analysis of 44 850 correlations: it can be seen that both raw and filtered data had $d$ values below critical significance threshold (vertical line), hence are providing wrong correlation estimates (99.6% for the raw and 100% for the filtered data). By contrast, 100% of the prewhitened data had $d$ values above the threshold, thus providing correct estimates.

*3.3.2. Neural connectivity maps.* Both fundamental statistical considerations (discussed in the introduction and section 4 below) as well as the results obtained above show that correlations between nonstationary and/or autocorrelated time series are spurious. In this analysis we assessed the extent of this error and the effect it may have on inferences about neural connectivity by plotting the neural connectivity pattern obtained by correlating filtered and prewhitened series.

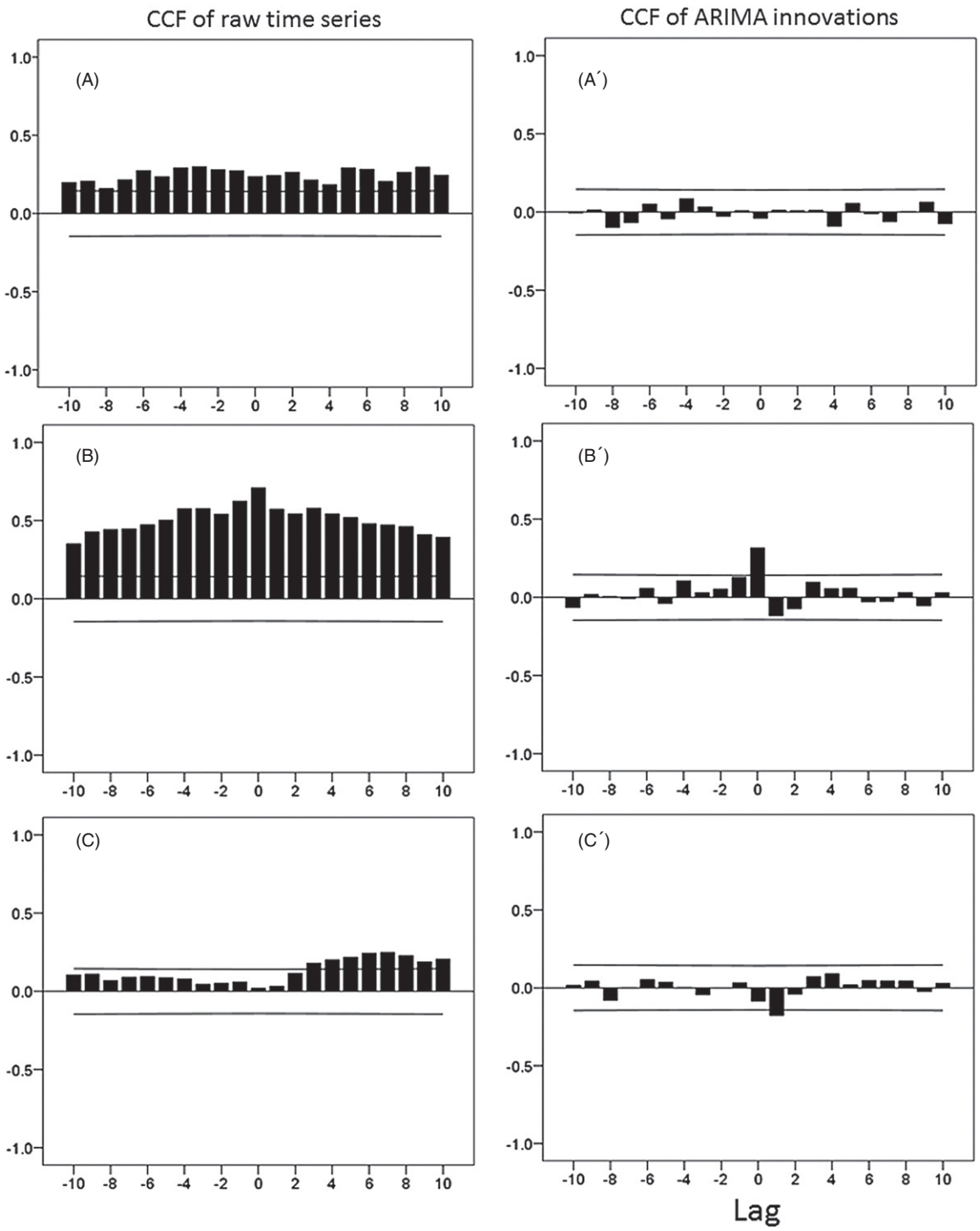


**Figure 5.** Three additional examples of spurious CCF (A, B, C) between raw time series and corresponding true CCF (A′, B′, C′) between the corresponding ARIMA innovations. Notice that the presence of a true significant CCF between innovations (C′) is missed in the raw series (C).

Figure 8 plots the spatial pattern of significant ($p < 0.05$) zero-lag correlations obtained for the right superior parietal lobule of one subject. As expected from first principles, the number of significant correlations was much higher (3.5 times) in the filtered than the prewhitened case. Even more importantly, it can be seen in figure 8 that the prewhitened analysis yielded an interesting pattern of functional connectivity within the superior parietal lobule, consisting of two separate subgroups linked by negative correlations; no such pattern was discernible in the filtered case. These results underscore the power and prospect of the correct correlation analysis for discovering true neural connectivity patterns. Very similar results were obtained for other areas and are currently under investigation.

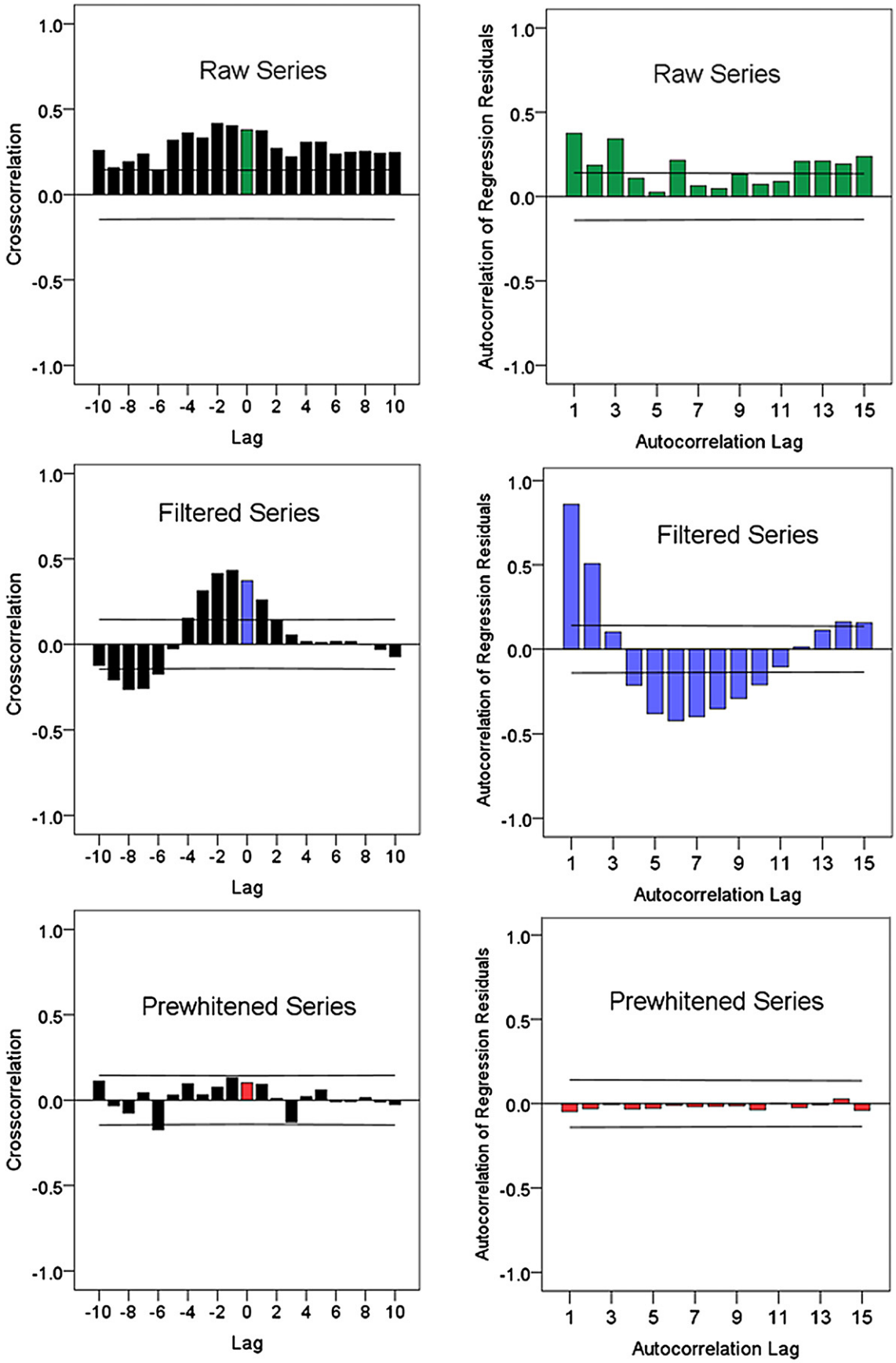


**Figure 6.** Left panel: crosscorrelograms of raw, filtered (see the text) and prewhitened BOLD time series of the same voxel pair. Right panel: color-coded autocorrelograms of the regression residuals for the zero-lag correlation.

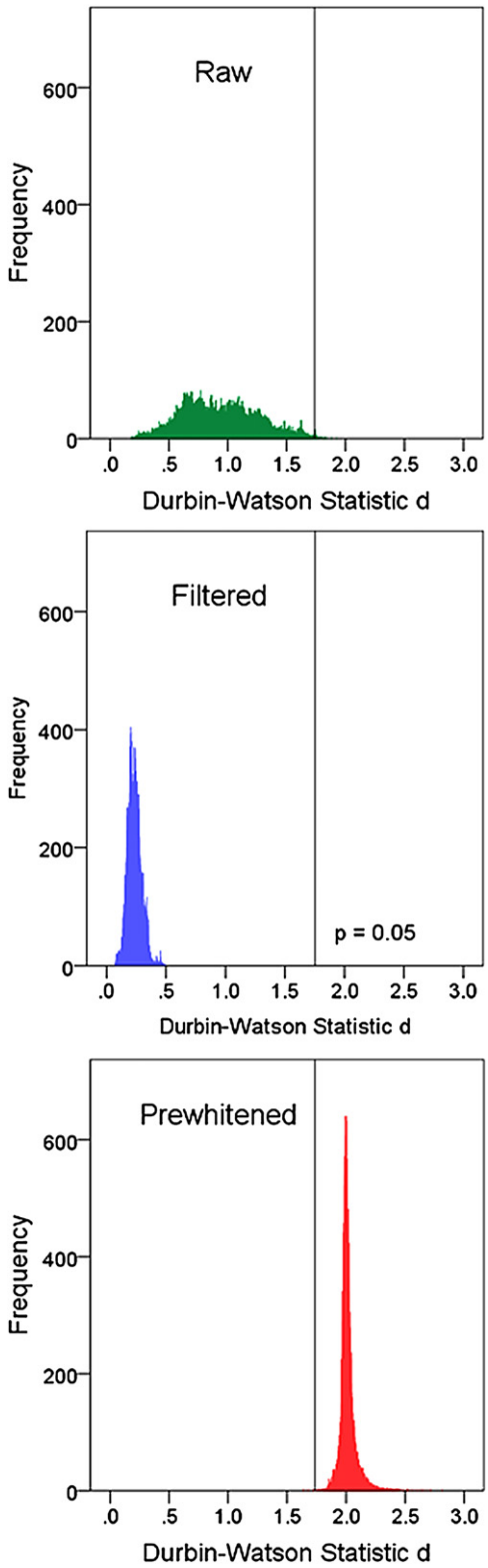


**Figure 7.** Frequency distributions of the Durbin–Watson $d$ statistic in 44 850 cases of zero-lag crosscorrelations (all pairwise correlations between 300 voxels). The vertical line indicates the $p < 0.05$ threshold for rejecting the null hypothesis that the serial correlation of the regression residuals is zero. Values below that level (i.e. to the left of the line) reject the null hypothesis (indicating that there exists a significant serial correlation).

### *3.4. Peak crosscorrelations*

*3.4.1. General.* As mentioned above, a crosscorrelogram was computed for each pair of voxels (0 lag ± 10 lags = 21 crosscorrelations). For this analysis, we wanted to identify the sign, magnitude and lag of the strongest crosscorrelation in each crosscorrelogram, and how these measures differed among the four brain groups defined above. For that purpose, the maximum absolute crosscorrelation was found and its sign and lag noted and assigned to one of the four brain groups, depending on the location of the crosscorrelated voxels. For each group, the following summary statistics were computed for each lag: (1) the number of positive crosscorrelations ($N_p$), (2) the number of negative crosscorrelations ($N_n$), (3) the positive/negative ratio: $\frac{N_p}{N_n}$, (4) the percentage of positive crosscorrelations (with respect to all positive crosscorrelations), (5) the percentage of negative crosscorrelations (with respect to all negative crosscorrelations), (6) the mean positive $z$-transformed crosscorrelation, (7) the mean negative $z$-transformed crosscorrelation, and (8) the overall $z$-transformed mean. We found the following.

*3.4.2. Sign and counts of peak crosscorrelations.* With respect to the counts of the strongest crosscorrelations, there were many more positive than negative crosscorrelations. Figure 9 shows the $\frac{N_p}{N_n}$ ratio as a function of lag for each group. (The positive and negative lags have been collapsed to their absolute value, since the sign of the lag has no meaning when averaging.) It can be seen that this ratio was very high at zero lag, decreased at |lag| = 1, and practically became unity for subsequent lags. In addition, there were systematic differences among the four brain groups, in that the $\frac{N_p}{N_n}$ ratio was highest for the intra-area group, and progressively lower for the homotopic, ipsi-hemispheric and contra-hemispheric groups. These group differences were most prominent at zero lag and at |lag| = 1. An ANOVA on $\log_e\left(\frac{N_p}{N_n}\right)$ (see section 2) showed highly significant effects of group ($F_{3,1468} = 9.72$, $P < 0.001$), |lag| ($F_{10,1468} = 537.39$, $P < 0.001$) and group ×|lag| interaction ($F_{30,1468} = 2.18$, $P = 0.002$).

*3.4.3. Lag distributions of peak crosscorrelations.* Positive and negative crosscorrelations were distributed unevenly across different lags. The percentage of positive (peak) crosscorrelations was highest at zero lag and decreased smoothly at longer lags, becoming practically flat at |lag| ⩾ 3 (figure 10, upper panel). In addition, there were systematic group differences; an ANOVA on the arcsin-transformed proportions (see section 2) showed highly significant effects of group ($F_{3,1468} = 8.95$, $P < 0.001$), |lag| ($F_{10,1468} = 1962.5$, $P < 0.001$) and group $x$|lag| interaction ($F_{30,1468} = 19.73$, $P < 0.001$). In contrast, the percentages of negative crosscorrelations varied more widely across lags (figure 10, lower panel), with a peak at |lag| = 2. An ANOVA showed a highly significant effect only of |lag| ($F_{10,1468} = 212.59$, $P < 0.001$); neither group nor the group ×|lag| interaction were statistically significant ($P = 0.982$ and $P = 0.999$, respectively). It can be seen in figure 10 (lower panel) that

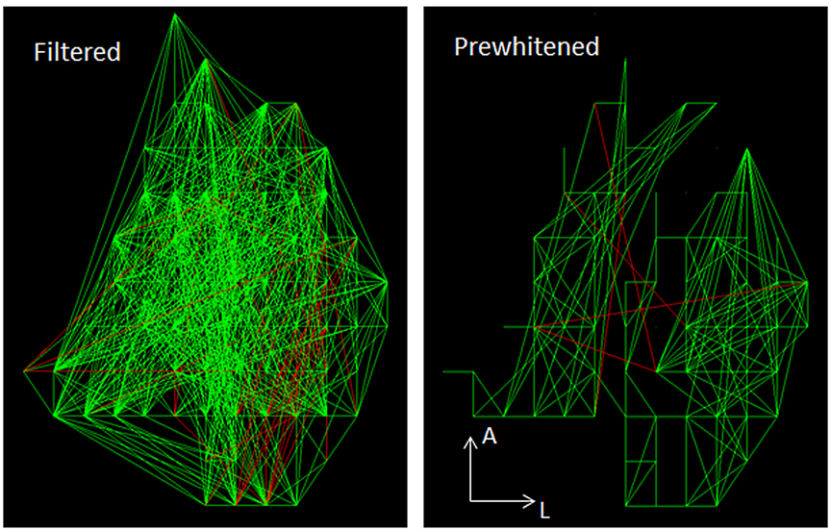


**Figure 8.** Network connectivity patterns of the right superior parietal lobule of a single subject derived using filtered (see the text) or prewhitened BOLD time series. Green and red lines indicate positive or negative zero-lag cross correlations, respectively. A nominal threshold of $p < 0.05$ on the correlation coefficient was applied. There were 3.5 times more significant correlations in the filtered than the prewhitened series ($N = 830$ and 241, respectively).

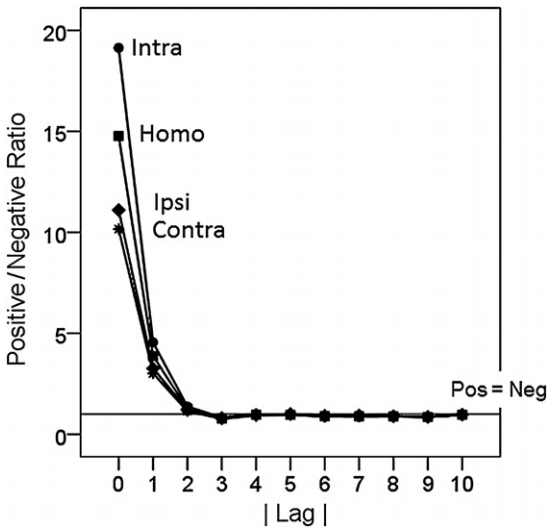


**Figure 9.** Positive/negative ratio of the counts of peak crosscorrelations for the four brain groups is plotted against the absolute lag.

the percentage for the ipsi- and contra-hemispheric groups (blue and magenta color, respectively, almost superimposed) are lower than the other values. To test whether this was significant, we performed an additional ANOVA specifically for $|\text{lag}| = 0$. The group effect was not statistically significant ($P = 0.873$); in addition, none of the pairwise comparisons between groups showed any statistically significant difference ($P > 0.5$ for all comparisons).

*3.4.4. Strength of peak crosscorrelations.* Figure 11 plots the mean ($z$-transformed, across subjects) crosscorrelations for different lags and groups. It can be seen that (a) positive crosscorrelations were consistently stronger (i.e. in absolute value) than negative ones, (b) both positive and negative crosscorrelations were strongest at zero lag and decreased progressively at longer lags, and (c) both positive and negative crosscorrelations were strongest for the intra-area group and progressively weaker for the homotopic, ipsi-hemispheric, and contra-hemispheric groups. Interestingly, the intra-area group seems to cluster with the homotopic group, whereas the ipsi-hemispheric group seems to cluster with the contra-hemispheric group. An ANOVA on positive crosscorrelations showed highly significant effects of group ($F_{3,1468} = 26.63$, $P < 0.001$), $|\text{lag}|$ ($F_{10,1468} = 441.48$, $P < 0.001$) and group $\times|\text{lag}|$ interaction ($F_{30,1468} = 22.0$, $P < 0.001$). An ANOVA on negative crosscorrelations showed highly significant effects of group ($F_{3,1468} = 107.78$, $P < 0.001$), $|\text{lag}|$ ($F_{10,1468} = 1175.4$, $P < 0.001$) and a weaker group $\times|\text{lag}|$ interaction ($F_{30,1468} = 1.59$, $P = 0.023$).

### *3.5. Zero-lag crosscorrelations*

*3.5.1. General.* In the previous section we focused on the analysis of peak crosscorrelations with respect to their values, sign, lag distribution and brain group differences. In this section we focused specifically on the crosscorrelations observed at zero lag, irrespective of the location of the peak crosscorrelation. These two analyses provide different and complementary information.

*3.5.2. Sign and counts of zero-lag crosscorrelations.* Overall, there were approximately three times more positive than negative correlations (figure 12); these proportions were highly statistically significant (paired $t$-test on arcsin-transformed proportions, $t_{71} = 33.29$, $P < 0.001$, $N = 18$ subjects $\times$ 4 groups = 72). In addition, there were systematic differences among the four brain groups, which are as follows (figure 13). With respect to the frequency of occurrence of positive and negative correlations, (a) the percentage of positive correlations was highest for the intra-area group,

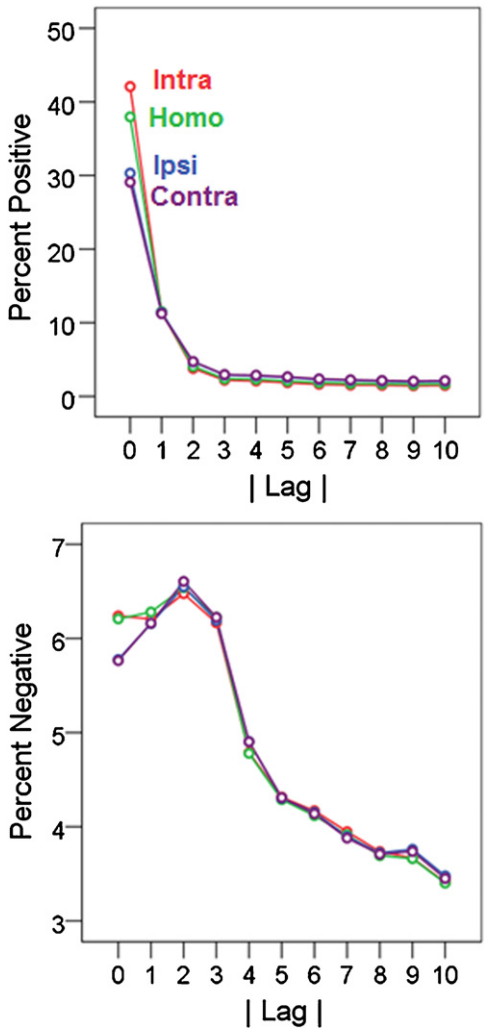


**Figure 10.** Relative distributions of positive (upper panel) and negative (lower panel) crosscorrelations are plotted against absolute lag for the four brain groups. Since the negative and positive were collapsed (see the text), 100% = percentage at zero lag + (2 × percentage at the other lags).

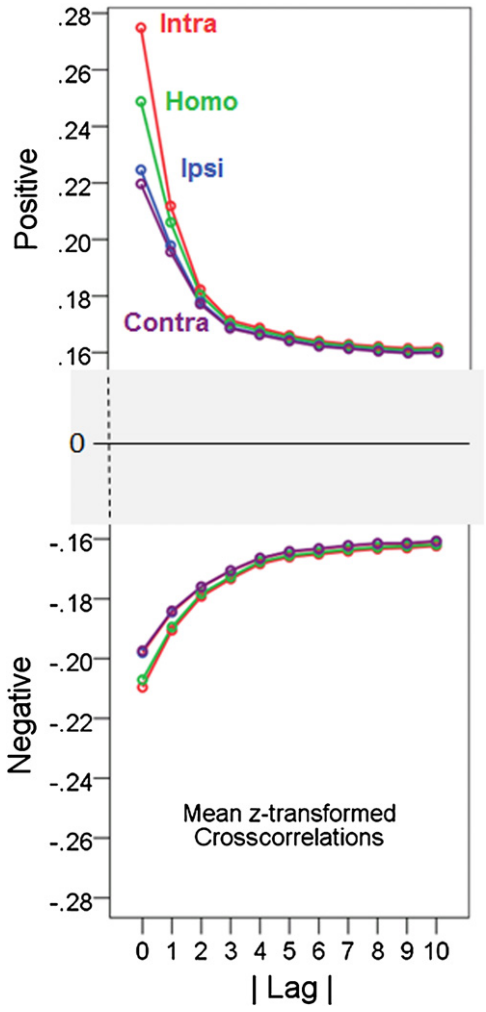


**Figure 11.** Mean $z$-transformed positive and negative crosscorrelations for each brain group are plotted against absolute lag.

and progressively lower for the homotopic, ipsi-hemispheric and contra-hemispheric groups (ANOVA, group main effect, $F_{3,68} = 6.14$, $P = 0.001$) (figure 13, top panel); (b) conversely, the percentage of negative correlations was lowest in the intra-area group, and progressively higher for the homotopic, ipsi-hemispheric and contra-hemispheric groups (ANOVA, group main effect, $F_{3,68} = 6.34$, $P = 0.001$) (figure 13, middle panel); (c) the positive/negative ratio was highest for the intra-area group, and progressively lower for the homotopic, ipsi-hemispheric and contra-hemispheric groups (ANOVA, group main effect, $F_{3,68} = 6.00$, $P = 0.001$) (figure 13, bottom panel).

*3.5.3. Strength of zero-lag crosscorrelations (figure 15).* Overall, the strength of the mean positive $z$-transformed zero-lag crosscorrelation ($z^0 = 0.13$) was approximately two times that of the mean negative one ($|z^0| = 0.07$) (figure 14). In addition, there were systematic differences among the four brain groups, which are as follows (figure 15). Specifically, the $z$-transformed mean positive crosscorrelation was highest for the intra-area group, and progressively lower for the homotopic, ipsi-hemispheric and contra-hemispheric groups (ANOVA, group main effect, $F_{3,68} = 13.83$, $P = 0.001$) (figure 15, top panel). In contrast, the $z$-transformed mean negative crosscorrelation did not differ significantly among groups (ANOVA, group main effect, $F_{3,68} = 0.974$, $P = 0.41$) although it was lowest in the intra-area group, and progressively higher for the homotopic, ipsi-hemispheric and contra-hemispheric groups (figure 15, middle panel). Finally, statistically significant differences with respect to brain groups were observed for the overall mean (ANOVA, group main effect, $F_{3,68} = 11.10$, $P < 0.001$).

*3.5.4. Relative brain groups contributions.* A different issue concerns the relative contributions of the various sources (i.e. the four brain groups) to the whole variance accounted for by them. We derived approximate estimates of these contributions as follows. First, we calculated the mean of the absolute values of the zero-lag $z$-transformed crosscorrelations for each group. This step ensured that all correlations are taken

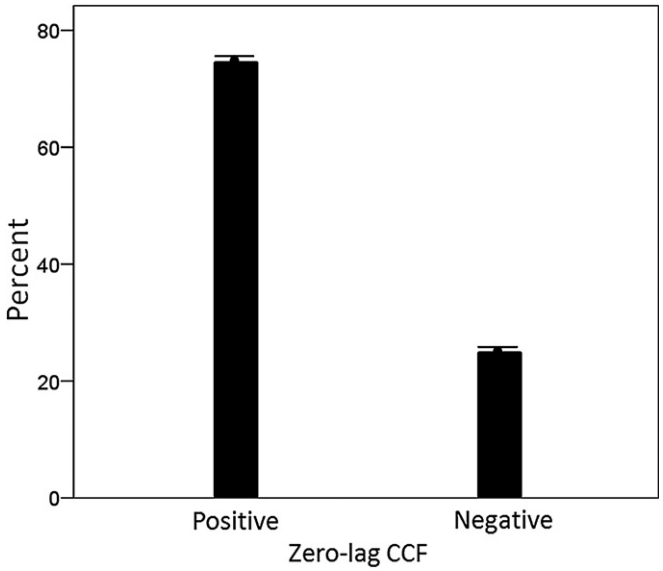


**Figure 12.** Percentages of positive and negative zero-lag crosscorrelations (total $N = 1255\,517\,520$). Lines on top of the bars indicate one SEM calculated from across subjects and brain groups ($N = 18$ subjects $\times$ 4 groups $= 72$).

into account, irrespective of their sign. Next, we converted these $z$-transformed values to crosscorrelations. Then, we squared these crosscorrelations to derive the proportion of variance accounted for by the crosscorrelation in each group. Finally, we added these proportions and re-expressed them as percentages of their sum. These percentages were 35% for the intra-area group, 27% for the homotopic group, 20% for the ipsi-hemispheric group, and 18% for the contra-hemispheric group (figure 16). These values can be considered as approximate estimates of the overall relative strength of association between zero-lag, BOLD voxel signals in the different brain groups.

## 4. Discussion

### *4.1. Methodological considerations*

*4.1.1. Spuriousness of correlating nonstationary autocorrelated time series.* As mentioned in the introduction, previous studies of functional connectivity have typically relied on correlating time series, variously preprocessed (e.g. filtered, adjusted, smoothed, averaged, etc) but without taking into consideration the single most important aspect in a time series, namely their internal structure (i.e. nonstationarity and autocorrelation). The point is that the true value of such results with respect to the true association between the two time series is undetermined, since the computed correlations variously reflect a combination of factors, including the internal structure of the series, external influences and the true relation between the two series [15]. Unless the time series being correlated are stationary and nonautocorrelated, their computed correlations will be spurious, due, among other reasons, to autocorrelated errors. It is this aspect which spoils any correlation between nonstationary and/or nonautocorrelated time series and which renders any conclusions drawn from such analysis invalid. To

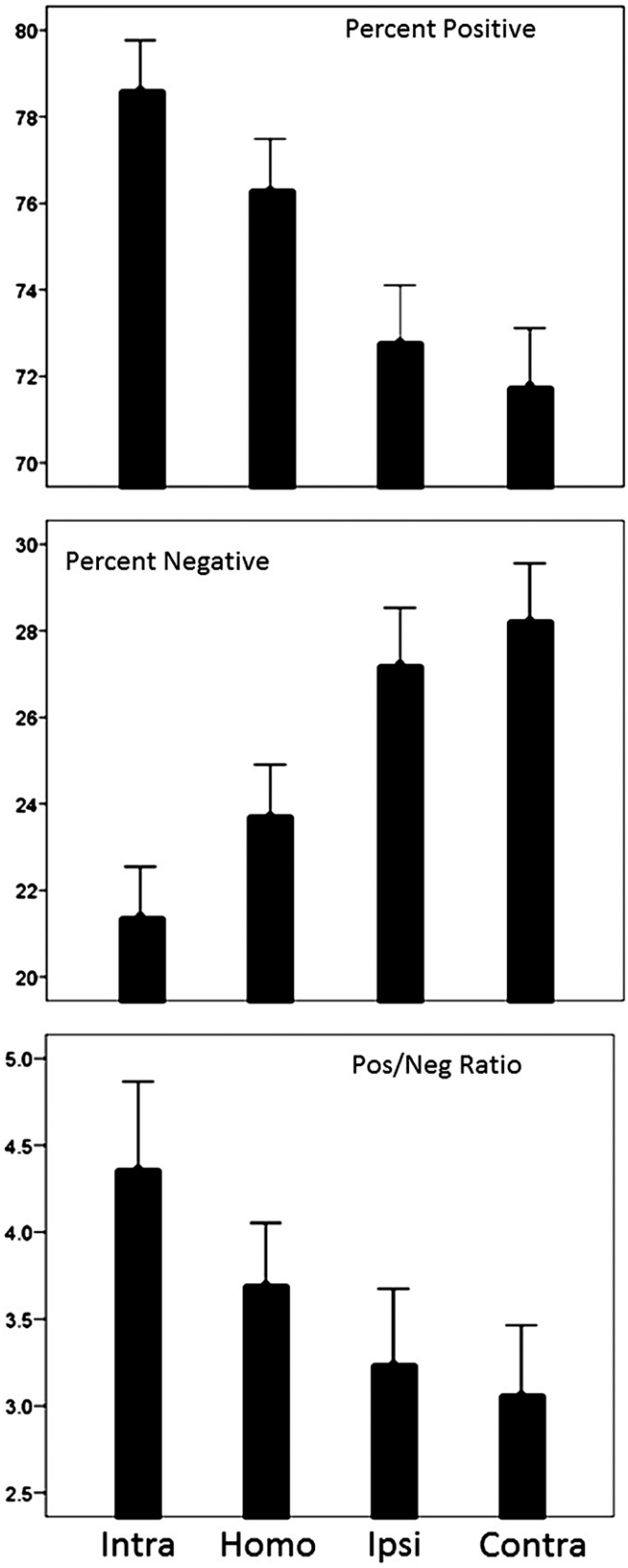


**Figure 13.** Mean percentages of positive, negative and positive/negative ratio of zero-lag crosscorrelations for each brain group, as indicated. Lines on top of the bars indicate one SEM calculated from across subjects ($N = 18$).

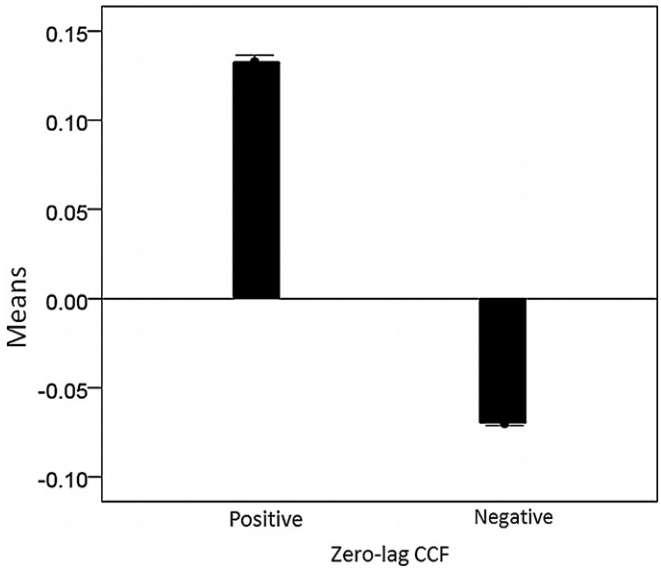


**Figure 14.** Mean positive, negative and overall $z$-transformed zero-lag crosscorrelations for each brain group, as indicated. Conventions as in figure 13

quote directly from a famous paper by Granger and Newbold [14] on work that was cited in the 2003 Clive Granger Nobel Prize press release [21] and discussed by Granger in his Nobel Prize lecture [20]:

'There are, in fact, as is well known, three major consequences of autocorrelated errors in regression analysis:

(i) Estimates of the regression coefficients are inefficient.
(ii) Forecasts based on the regression equations are sub-optimal.
(iii) The usual significance tests on the coefficients are invalid' ([14], p 111).

In fact, the detrimental effects of correlated errors has been stressed repeatedly over the past several decades with respect to regression in general [7, 8], correlation of raw time series [10, 12–18], and forecasting in single time series [16]. And yet, all studies we know of on resting or task-related fMRI during the past 16 odd years have relied on correlations between raw (or filtered) nonstationary and/or autocorrelated time series. (Those studies are too many to cite here; for typical examples, see [4] and [45] for resting and task fMRI studies, respectively.) The current situation in our field resembles very much the situation in econometrics in the early 1970s. It is worth quoting again from the paper of Granger and Newbold [14], published 37 years ago: 'We find it very curious that whereas virtually every textbook on econometric methodology contains explicit warnings of the dangers of autocorrelated errors, this phenomenon crops up so frequently in applied work' ([14], p 111).

The same considerations apply to time series analyses in the frequency (spectral) domain, since the two methods (time and frequency domains) are intimately related [9]. For example, the autospectrum is the Fourier transform of the autocovariance function, and, similarly, the cross spectrum is the Fourier transform of the crosscovariance function.

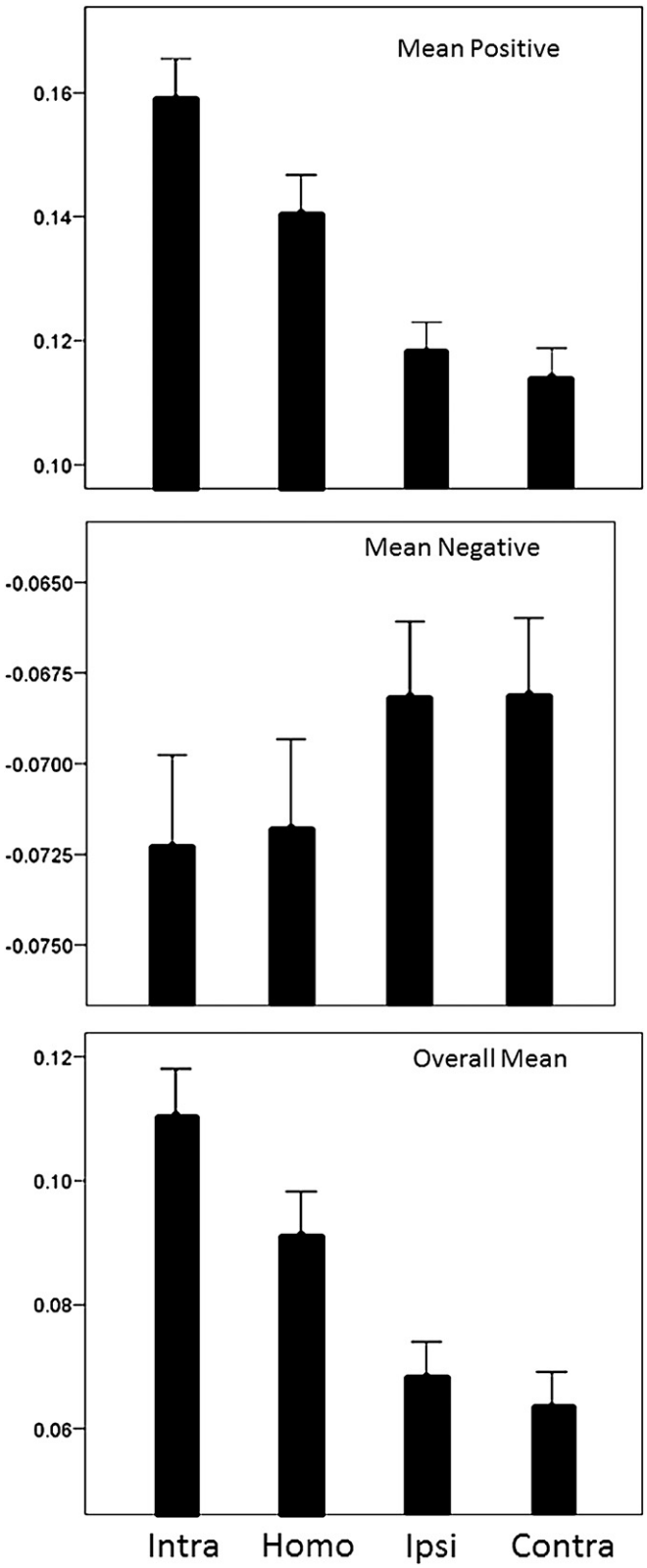


**Figure 15.** Mean positive and negative zero-lag $z$-transformed crosscorrelations across all brain groups. Conventions as in figure 13.

Spectral analyses of times series have a long history (see, e.g., [9, 18, 46–49]. All of this early work, as well as subsequent work, has drawn attention to the detrimental effects of

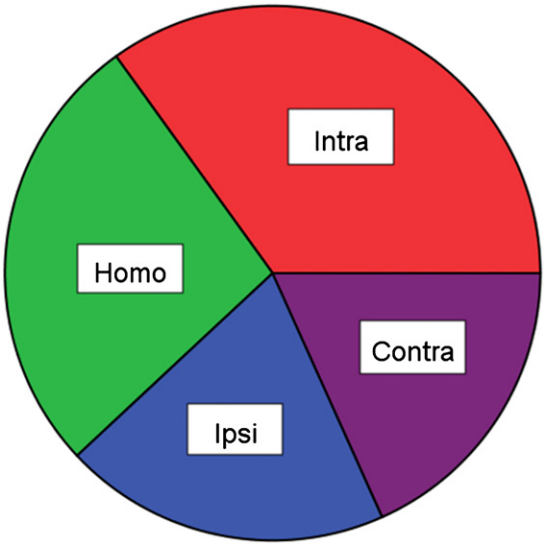


**Figure 16.** Relative contributions of the four brain groups to the zero-lag crosscorrelations (see the text for details).

nonstationarities and autocorrelations on estimating the true spectral coherency between two time series. We quote directly from Jenkins and Watts [9]: for the time domain: '... unless a filtering operation is applied to both series to convert them to white noise, spurious cross correlations may arise' ([9], p 321); and for the frequency domain: '... the sample phase and cross amplitude spectral estimators are derived, under the assumption that the two processes are uncorrelated white noise processes' ([9], p 363). The choice of the specific method to use depends on the problem; for example, frequency domain analyses (i.e. cross spectral analyses) yield valuable information on relations between the two series across a range of frequencies, whereas time domain analyses (i.e. CCF) provide valuable information on the sign (positive or negative) of the relation. In fact, time-domain and frequency-domain analyses can be used profitably on the same problem ([9], p 367). However, the important point is that for valid inferences to be obtained regarding the relations between two time series, both methods require that the time series be stationary and nonautocorrelated.

*4.1.2. Prewhitening.* To find the true relation between two time series, a two-stage approach is followed, explicated lucidly in [15]. First, univariate models are fitted to each series and the residuals (innovations) taken, to strip the series of nonstationarities and autocorrelations before a correlation (or coherence) is computed. Thus the series are converted to white noise [14–16], and hence the term 'prewhitening' [46] (see also [49]). Prewhitening can be achieved either in the frequency domain [46, 47] or in the time domain [10, 25]. The latter procedure is called ARIMA [10], a term derived from the initials of three essential components that define a time series, namely an AutoRegressive component (i.e. the dependence of a given value in the series on previous values), an Integrative component (e.g. a linear trend), and a Moving Average component (i.e. the dependence of a given value on random shocks of previous values). This procedure is standard in time series analysis, is straightforward, is described in many time series analysis textbooks [10, 18, 22–25], and is readily implemented in various statistical packages (e.g. SPSS, Matlab, SAS, R, etc). The main tool for model identification is the autocorrelation and partial autocorrelation functions, assuming that the series is suitably differenced to be stationary. In the frequency domain, the tool is the spectrum which is the Fourier transform of the autocorrelation function of the differenced (stationary) series. Prewhitening is a standard procedure in many fields, especially in industrial engineering and econometrics, where forecasting and control carry major weight and where wrong statements and predictions carry substantial penalties.

*4.1.3. Other approaches.* Crosscorrelation analyses in fMRI research address directly the issue of dynamic connectivity; in contrast, the grouping of fMRI time courses into similar patterns addresses the issue of similarity of spontaneous or evoked temporal fluctuations in the BOLD signal. It should be noted that these are two very different issues: (a) no inferences on connectivity can be drawn from similarities in time courses, whereas, conversely, (b) no inferences on similarity of time courses can be drawn from information on connectivity. The former case is undetermined, since many different quantities can have very similar time courses without been connected (e.g. trains moving north with the same speed time course in Paris and Athens); and in the latter case, the relation between the time courses in a pair of connected quantities is determined by their transfer function (including feedback and delays), and may or may not be similar.

Grouping of fMRI time courses according to their shape has been carried out using principal component analysis (PCA) and independent component analysis (ICA) (see recent reviews [2, 3]). These methods have provided useful information concerning neural systems participating in potentially common functions. However, as mentioned above, no inference on connectivity can be drawn from the degree of similarity of time courses, and, hence, no such inferences on neural connectivity can be drawn from PCA or ICA analysis of BOLD time courses. Problems arise when correlations are computed between BOLD time series grouped together by prior PCA or ICA analyses (see [50] for an example): such correlations are spurious if the raw (or filtered) data are used, as discussed above. The point is that the selection process of which time series are being correlated is irrelevant to the correlation itself: it makes no difference whether the two series are from the same or different ICA-based groups. The only aspect that matters is whether the series are stationary and nonautocorrelated in order for the correlations obtained to be correct (i.e. not to be spurious). In fact, any grouping method, including PCA, ICA or other, could be very useful if coupled with proper crosscorrelation analysis of prewhitened series.

### *4.2. Peak crosscorrelations across lags*

In this study we carried out an extensive analysis of voxel-by-voxel pairwise crosscorrelations after each series was prewhitened to yield stationary, nonautocorrelated

innovations. Therefore, the estimates of the interactions (i.e. crosscorrelations) obtained reflect the true associations between voxel BOLD time series and are not spurious. As a first step for this analysis, we focused on crosscorrelations of voxels within the same area, between homotopic areas, between an area and all other voxels in the same hemisphere, and between an area and all voxels in the contralateral hemisphere (excluding the homotopic area). As shown in figure 5, individual crosscorrelograms varied widely in shape. In order to evaluate their basic aggregate characteristics, we focused on the peak (i.e. highest absolute value) of the crosscorrelogram: analyzing the peaks enabled us to derive summary statistics on the highest possible interactions between single voxel BOLD time series. We performed analyses extending up to 10 lags (i.e. 20 s, given TR = 2 s), as an upper limit of expected interactions, and collapsed the positive and negative sides of the crosscorrelogram, since the sign of the lag has no meaning in pooled data. We then analyzed the prevalence of positive and negative crosscorrelations, and their strength, as a function of the lag (figures 9–11). There were five major findings. First, positive interactions were much more frequent and stronger than negative ones; second, the strongest interactions (mean absolute values of crosscorrelations, figure 11) occurred at zero lag and decreased gradually at longer lags; third, the strength of interactions varied systematically with the brain group, such that intra-area > homotopic > ipsi-hemispheric > contra-hemispheric; fourth, the relative distribution of positive interactions had a peak at zero lag, declined progressively at longer lags, and differed among brain groups in the same order as above; and fifth, and in contrast to the positive interactions, the relative distribution of negative interactions had a peak (tuned) at |lag| = 2 and did not differ significantly among brain groups. We discussed these findings in that sequence below.

These findings validate the resting, task-free BOLD signal as reflecting neural activity, since it is difficult to see how else this BOLD signal could be correlated between voxels of areas far away, such as homotopic areas in opposite hemispheres. The finding that positive interactions occurred more frequently and were stronger than negative ones is not surprising, as it most probably reflects the more widespread excitatory effects in the cerebral cortex. For example, all long-range corticocortical projections are excitatory, whereas inhibitory mechanisms are local and, even there, more limited than the excitatory ones. Also, the high percentages and values at zero lag are in accord with other findings [33] and are discussed in more detail below. Perhaps the most remarkable findings of this analysis are (a) the discovery of the tuning of the negative interactions at |lag| = 2, i.e. at a relative shift of the time series by 4–6 s (given TR = 2 s), and (b) the fact that this tuning was invariant across all four brain groups. We interpret this finding as reflecting the localized and uniform nature of cortical inhibitory mechanisms, namely that such mechanisms are local and of the same nature and similar circuitry in various cortical areas, hence the invariance across groups.

### *4.3. Zero-lag crosscorrelations*

Interactions at zero lag (i.e. within an interval of TR = 2 s) are a special case for two reasons. First, because they were most prevalent (as compared to other lags, see above) and second because synchronicity is a principle of brain function in its own merit. In this analysis, we focused on zero-lag crosscorrelations as a time-snapshot, so to speak, irrespective of the location of the crosscorrelogram peak. We found an orderly variation of zero-lag crosscorrelations with respect to their sign, strength and dependence on brain groups. This indicates a robust underlying organization of synchronous variation in resting neural activity. As pointed out in the discussion of the results from recent studies using magnetoencephalography (MEG) [32–36], the four most likely sources of synchronization include recurrent axon collaterals of pyramidal cells [51], specific (parvalbumin) thalamocortical afferents [52, 53], divergent, multifocal (calbindin) thalamocortical afferents [52], and broadly distributed noradrenergic fibers [54]. In addition, since BOLD measurements were taken every 2 s in this study, it is likely that corticocortical interactions with some lag (in the order of milliseconds) also contribute. It is interesting that the sign of correlation also varied in a systematic fashion across the four brain groups, with the proportion of negative correlations increasing from group I to group IV. This could reflect the similarity in the kind of information being processed. For example, within an area (group I), negative interactions are low because local cell ensembles perform similar operations; hence, they positively cooperate. This would also hold, but to a lesser extent, for interactions between a given area and its homotopic area in the opposite hemisphere (group II). In contrast, other areas in the same hemisphere (group III), and certainly other areas in the opposite hemisphere (group IV) would be involved in their own information processing; hence, they may be not expected to cooperate (i.e. positively correlated) with that given area. Such considerations would explain as follows the orderly trends observed for the variation of the percentage of positive and negative crosscorrelations across brain groups. The fact that the positive/negative ratio is always greater than 1 (i.e. the number of positive crosscorrelations is greater than the negative ones) underscores the greater preponderance of excitatory (versus inhibitory) mechanisms in the cerebral cortex, as discussed above. However, the orderly decrease of that ratio across intra-area, homotopic, ipsi-hemispheric and contra-hemispheric groups, in that order, suggests a different operating principle which, we propose, reflects the similarity of information being processed. In that sense, the categorical brain group horizontal axis in figure 13 would correspond to a qualitative axis of similarity in information processing. This idea can be further tested by analyzing data from specific areas, a work in progress in our laboratory.

Overall, these results indicate an orderly variation in synchronicity that seems to closely reflect the presence and density of direct anatomical connections, an idea also suggested by other investigators (see, e.g., [55–59]). These are most dense within an area, substantial across homotopic areas and sparse across heterotopic areas (see, e.g., [60]).

The covariation in activity comes from the fact that these connections are typically reciprocal, leading to a practically synchronous (within the 2 s of fMRI TR time) activation between interconnected areas. Thus, there may be nothing special about 'default' networks [see 2, 3] beyond their reflection of existing anatomical connectivity.

Finally, our analysis provided an approximate quantitative assessment of the relative contributions of the different kinds of brain groups (figure 16), as defined based on known anatomical connectivity. These relative contributions are broad estimates derived from averaging large numbers of crosscorrelations. It is reasonable to suppose that interactions are actually spatially specific, in which case our measurements are likely to underestimate such spatially restricted interactions. We are currently investigating this issue by analyzing the fine-grain spatial distribution of the crosscorrelations obtained (see figure 8 for an example).

### *4.4. State of the field: spurious correlations in functional neuroimaging and what needs to be done*

Talk about spurious or nonsense correlations between time series dates at least 85 years back, when G Udny Yule delivered the Presidential Address at the 1925–26 session of the Royal Statistical Society in a lecture titled 'Why do we sometimes get nonsense-correlations between time-series?' [61]. His famous example was the high positive correlation of 0.9512 between the proportion of Church of England marriages to all marriages for the years 1866–1911 and the standardized mortality per 1000 persons for the same years. Yule had the following comment on this finding: 'Now I suppose it is possible, given a little ingenuity and goodwill, to rationalize very nearly anything. And I can imagine some enthusiast arguing that the fall in the proportion of Church of England marriages is simply due to the Spread of Scientific Thinking since 1866, and the fall in mortality is also clearly to be ascribed to the Progress of Science; hence both variables are largely or mainly influenced by a common factor and consequently ought to be highly correlated. But most people would, I think, agree with me that the correlation is simply sheer nonsense; that it has no meaning whatever; that it is absurd to suppose that the two variables in question are in any sort of way, however indirect, causally related to one another' ([61], p 2). Yule astutely located the problem to the autocorrelations of the time series, and explored ways for correct analyses using techniques similar to modern prewhitening. Since Yule's lecture, the topic of spurious regressions resurfaced with force in applied economics, leading to a false (spurious) prediction [11], its refutation using prewhitening [12], a simulation study [14], and a textbook [16]. By the end of the 1970s, the matter of how to analyze correctly relations between time series had been settled in statistics and econometrics.

Now, this issue became prominent in functional neuroimaging in the 1990s [62] and has continued to be in the foreground up to now unabated. As discussed above, a large number of studies have been carried out in which correlations between raw (or filtered, averaged, etc) BOLD (and MEG [63]) time series have been performed as the main tool to investigate dynamic, neural connectivity. Now, it is common practice in these studies to correlate BOLD time series in the resting or task-driven state without paying attention to the serious errors in the correlations obtained due to autocorrelated residuals. This can be tested rigorously by (a) plotting the autocorrelogram of these residuals, and (b) calculating the Watson–Durbin test statistic [43]. Unfortunately, to our knowledge, no such information has been provided in the literature. Given the known nonstationarity and autocorrelation of BOLD time series, it is obvious that correlations between such series are spurious [12, 14, 16]. The reason why 'default' brain networks inferred from such correlations may be found to be in accord with known anatomical connectivity stems from the fact that an existing, true relationship is part of the equation but its relative contribution is undetermined due to the influence of nonstationarity and autocorrelation present in the individual series. It is remarkable that history repeats itself and that essentially we are facing the same problem that the field of econometrics faced 40 years earlier [12, 14, 16]. Indeed, we may paraphrase without loss of generality Granger and Newbold's comment in 1974 [14]: We find it very curious that whereas virtually every textbook on time series methodology contains explicit warnings of the dangers of autocorrelated errors, this phenomenon crops up so frequently in functional neuroimaging work.

Be that as it may, it is instructive to note how that problem was dealt with in the field of econometrics when the flaws of regression analysis with autocorrelated errors were exposed. The best and most succinct exposition was given by Granger in his 2003 Nobel Prize Lecture. He said:

> An example is a problem known as 'spurious regressions.' It had been observed, by Paul Newbold and myself in a small simulation published in 1974, that if two independent integrated series were used in a regression, one chosen as the 'dependent variable' and the other the 'explanatory variable,' the standard regression computer package would very often appear to 'find' a relationship whereas in fact there was none. That is, standard statistical methods would find a 'spurious regression.' *This observation lead to a great deal of reevaluation of empirical work, particularly in macroeconomics, to see if apparent relationships were correct or not. Many editors had to look again at their list of accepted papers.* Putting the analysis in the form of an error-correction model resolves many of the difficulties found with spurious regression. ([20], italics ours)

It seems appropriate and timely that such a reevaluation be carried out in the field of neuroscience. Reporting the Durbin–Watson statistic and providing the autocorrelogram of the regression residuals will clear the issue for a particular study, and prewhitening the time series will lead to the construction of brain network models, including 'default' networks, based on true, not spurious, correlations.

## Acknowledgments

This work was supported by United States Public Health Service grant NS32919 and the United States Department of Veterans Affairs.

*Note added in proof.* It is frequently thought that the problems stemming from autocorrelated BOLD time series can be dealt with by adjusting degrees of freedom (see, for example, [4] p 9674). This is incorrect. Specifically, the reference by Fox *et al* [4] to Bartlett's theory is misapplied. Bartlett's general asymptotic expression for the variance of the sample crosscorrelation coefficient assumes explicitly two jointly stationary time series with independent, identically distributed normal errors ([64]). As discussed above, the basic problem stems from serially correlated regression residuals, i.e. from the violation of the assumption of error independence in least squares regression, and not from the number of degrees of freedom; no adjustment of degrees of freedom can correct for serially correlated residuals. In addition, most problems in the literature stem from correlating integrated BOLD time series (i.e. time series with trends), in addition to their autocorrelation. Again, it is not a matter of *p*-value but the fact that in such cases the magnitude of the correlation itself and even the shape of the whole crosscorrelogram are suspect [16].

## References

[1] Biswal B, Yetkin F Z, Haughton V M and Hyde J S 1995 Functional connectivity in the motor cortex of resting human brain using echo-planar MRI *Magn. Reson. Med.* **34** 5370–41

[2] Cole D M, Smith S M and Beckmann C F 2010 Advances and pitfalls in the analysis and interpretation of resting-state FMRI data *Front. Syst. Neurosci.* **4** 8

[3] van den Heuvel M P and Hulshoff Pol H E 2010 Exploring the brain network: a review on resting-state fMRI functional connectivity *Eur. J. Neuropsychopharmacol.* **20** 519–34

[4] Fox M D, Snyder A Z, Vincent J L, Corbetta M, Van Essen D C and Raichle M E 2005 The human brain is intrinsically organized into dynamic, anticorrelated functional networks *Proc. Natl Acad. Sci. USA* **102** 9673–8

[5] Fox M D, Zhang D, Snyder A Z and Raichle M E 2009 The global signal and observed anticorrelated resting state brain networks *J. Neurophysiol.* **101** 3270–83

[6] Murphy K, Birn R M, Handwerker D A, Jones T B and Bandettini P A 2009 The impact of global signal regression on resting state correlations: Are anti-correlated networks introduced? *Neuroimage* **44** 893–905

[7] Box G E P, Hunter W G and Hunter J S 1978 *Statistics for Experimenters* (New York: Wiley)

[8] Draper N R and Smith H 1981 *Applied Regression Analysis* 2nd edn (New York: Wiley)

[9] Jenkins G M and Watts D G 1968 *Spectral Analysis and Its Applications* (Oakland, CA: Holden-Day)

[10] Box G E P and Jenkins G M 1970 *Time Series Analysis: Forecasting and Control* (San Francisco: Holden-Day)

[11] Coen P J, Gomme E D and Kendall M G 1969 Lagged relationships in economic forecasting *J. R. Stat. Soc.* A **132** 133–63

[12] Box G E P and Newbold P 1971 Some comments on a paper of Coen, Gomme and Kendall *J. R. Stat. Soc.* A **134** 229–40

[13] Priestley M B 1971 Fitting relationships between time series *Bull. Inst. Int. Stat.* **38** 1–27

[14] Granger C W J and Newbold P 1974 Spurious regressions in econometrics *J. Econometrics* **2** 111–20

[15] Haugh L D 1976 Checking the independence of two covariance-stationary time series: a univariate residual cross-correlation approach *J. Am. Stat. Assoc.* **71** 378–85

[16] Granger C W J and Newbold P 1977 *Forecasting Economic Time Series* (New York: Academic)

[17] Pierce D A 1979 $R^2$ measures for time series *J. Am. Stat. Assoc.* **74** 901–10

[18] Priestley M B 1981 *Spectral Analysis and Time Series* (San Diego, CA: Academic)

[19] Schwartz A B and Adams J L 1995 A method for detecting the time course of correlation between single-unit activity and EMG during a behavioural task *J. Neurosci. Methods* **58** 127–41

[20] Granger CWJ 2004 Time series analysis, cointegration, and applications. Nobel Prize Lecture 2003 *The Nobel Prizes 2003* ed T Frängsmyr (Stockholm, Sweden: Nobel Foundation) pp 360–6

[21] Nobel Prize in Economic Sciences, Press Release, 8 October 2003 Statistical methods for economic time series The Royal Swedish Academy of Sciences. http://nobelprize.org/nobel_prizes/economics/laureates/2003/press.html

[22] Vandaele W 1983 *Applied Time Series and Box–Jenkins Models* (San Diego, CA: Academic)

[23] Pankratz A 1991 *Forecasting with Dynamic Regression Models* (New York: Wiley)

[24] Yafee R and McGee M 2000 *Introduction to Time Series Analysis and Forecasting* (San Diego, CA: Academic)

[25] Box G E P, Jenkins G M and Reinsel G C 2008 *Time Series Analysis: Forecasting and Control* 4th edn (Hoboken, NJ: Wiley)

[26] Tagaris G A, Kim S-G, Ugurbil K and Georgopoulos A P 1995 Box–Jenkins intervention analysis of functional MRI data *3rd Scientific Meeting, and European Society for Magnetic Resonance in Medicine and Biology, 12th Annu. Meeting (Nice, France, 19–25 August 1995)* p 814

[27] Tagaris G A, Richter W, Kim S-G and Georgopoulos A P 1997 Box–Jenkins intervention analysis of functional magnetic resonance imaging data *Neurosci. Res.* **27** 289–94

[28] Locascio J J, Jennings P J, Moore C I and Corkin S 1997 Time series analysis in the time domain and resampling methods for studies of functional magnetic resonance brain imaging *Hum. Brain Mapp.* **15** 168–93

[29] Georgopoulos A P, Christova P S, Lewis S M, Slagle E and Ugurbil K 2005 Co-processing of mental rotation and memory scanning in the brain: a voxel-by-voxel analysis of 4 Tesla fMRI activation *35th Annu. Meeting of the Society for Neuroscience (Washington, DC, 12–16 November 2005)* 640.16

[30] Georgopoulos A P, Christova P S and Lewis S M 2006 Functional network analysis of brain areas using fMRI in four cognitive tasks *36th Annu. Meeting of the Society for Neuroscience (Atlanta, GA, 14–18 October 2006)* 262.16

[31] Lewis S M, Jerde T A, Goerke U, Ugurbil K and Georgopoulos A P 2006 Functional network analysis of superior parietal lobule (SPL) in two spatial cognitive tasks using fMRI at 7 Tesla *36th Annu. Meeting of the Society for Neuroscience (Atlanta, GA, 14–18 October 2006)* 262.8

[32] Leuthold A C, Langheim F J P, Lewis S M and Georgopoulos A P 2005 Time series analysis of magnetoencephalographic (MEG) data during copying *Exp. Brain Res.* **164** 211–22

[33] Langheim F J, Leuthold A C and Georgopoulos A P 2006 Synchronous dynamic brain networks revealed by magnetoencephalography *Proc. Natl Acad. Sci. USA* **103** 455–9

[34] Georgopoulos A P *et al* 2007 Synchronous neural interactions assessed by magnetoencephalography: a functional biomarker for brain disorders *J. Neural Eng.* **4** 349–55

[35] Georgopoulos A P, Tan H-M, Lewis S M, Leuthold A C, Winskowski A M, Lynch J K and Engdahl B 2010 The synchronous neural interactions test as a functional neuromarker for post-traumatic stress disorder (PTSD): a robust classification method based on the bootstrap *J. Neural Eng.* **7** 16011

[36] Engdahl B, Leuthold A C, Tan H-M, Lewis S M, Winskowski A M, Dikel T N and Georgopoulos A P 2010 The synchronous neural interactions test as a functional neuromarker for post-traumatic stress disorder (PTSD): a robust classification method based on the bootstrap *J. Neural Eng.* **7** 066005

[37] Talairach J and Tournoux P 1988 *Co-planar Stereotaxic Atlas of the Human Brain* (New York: Thieme)

[38] Kim S G, Hendrich K, Hu X, Merkle H and Ugurbil K 1994 Potential pitfalls of functional MRI using conventional gradient-recalled echo techniques *NMR Biomed.* **7** 69–74

[39] Lancaster J L, Rainey L H, Summerlin J L, Freitas C S, Fox P T, Evans A C, Toga A W and Mazziotta J C 1997 Automated labeling of the human brain: a preliminary report on the development and evaluation of a forward-transform method *Hum. Brain Mapp.* **5** 238–42

[40] Lancaster J L, Woldorff M G, Parsons L M, Liotti M, Freitas C S, Rainey L, Kochunov P V, Nickerson D, Mikiten S A and Fox P T 2000 Automated Talairach Atlas labels for functional brain mapping *Hum. Brain Mapp.* **10** 120–31

[41] Snedecor G W and Cochran W G 1989 *Statistical Methods* (Ames, IO: Iowa State University Press)

[42] Fisher R A 1958 *Statistical Methods for Research Workers* 13th edn (Edinburgh: Oliver and Boyd)

[43] Durbin J and Watson G S 1951 Testing for serial correlation in least squares regression: II *Biometrica* **38** 159–77

[44] von Neumann J 1941 Distribution of the ratio of the mean square successive difference to the variance *Ann. Math. Stat.* **12** 367–95

[45] Just M A, Cherkassky V L, Keller T A and Minshew N J 2004 Cortical activation and synchronization during sentence comprehension in high-functioning autism: evidence of underconnectivity *Brain* **127** 1811–21

[46] Press H and Tukey J W 1956 Power spectral methods of analysis and their application to problems in airplane dynamics *Flight Test Manual* NATO, Advisory Group for Aeronautical Research and Development pp 1–41

[47] Blackman R B and Tukey J W 1959 *The Measurement of Power Spectra from the Point of View of Communications Engineering* (New York: Dover)

[48] Granger C W J and Hatanaka M 1964 *Spectral Analysis of Economic Time Series* (Princeton, NJ: Princeton University Press)

[49] Brillinger D R 2002 John W Tukey's work on time series and spectrum analysis *Ann. Stat.* **30** 1595–618

[50] Kiviniemi V, Kantola J H, Jauhiainen J, Hyvarinen A and Tervonen O 2003 Independent component analysis of nondeterministic fMRI signal sources *Neuroimage* **19** 253–60

[51] Stefanis C and Jasper H 1964 Recurrent collateral inhibition in pyramidal tract neurons *J. Neurophysiol.* **27** 855–77

[52] Jones E G 2001 The thalamic matrix and thalamocortical synchrony *Trends Neurosci.* **24** 595–601

[53] Bruno R M and Sakmann B 2006 Cortex is driven by weak but synchronously active thalamocortical synapses *Science* **312** 1622–7

[54] Morrison J H, Molliver M E and Grzanna R 1979 Noradrenergic innervation of cerebral cortex: widespread effects of local cortical lesions *Science* **205** 313–6

[55] Honey C J, Kotter R, Breakspear M and Sporns O 2007 Network structure of cerebral cortex shapes functional connectivity on multiple time scales *Proc. Natl Acad. Sci. USA* **104** 10240–5

[56] Honey C J, Sporns O, Cammoun L, Gigandet X, Thiran J P, Meuli R and Hagmann P 2009 Predicting human resting-state functional connectivity from structural connectivity *Proc. Natl Acad. Sci. USA* **106** 2035–40

[57] Greicius M D, Supekar K, Menon V and Dougherty R F 2008 Resting-state functional connectivity reflects structural connectivity in the default mode network *Cereb. Cortex* **19** 72–8

[58] Hagmann P, Cammoun L, Gigandet X, Meuli R, Honey C J, Wedeen V J and Sporns O 2008 Mapping the structural core of human cerebral cortex *PLoS Biol.* **6** e159

[59] van den Heuvel M P, Mandl R C, Luigjes J and Hulshoff Pol H E 2008 Microstructural organization of the cingulum tract and the level of default mode functional connectivity *J. Neurosci.* **28** 10844–51

[60] Hedreen J C and Yin T C 1981 Homotopic and heterotopic callosal afferents of caudal inferior parietal lobule in Macaca mulatta *J. Comp. Neurol.* **197** 605–21

[61] Yule G U 1926 Why do we sometimes get nonsense-correlations between time-series?—a study in sampling and the nature of time-series *J. R. Stat. Soc.* **89** 1–63

[62] Friston K J, Jezzard P and Turner R 1994 Analysis of functional MRI time-series *Hum. Brain Mapp.* **2** 69–78

[63] de Pasquale F *et al* 2010 Temporal dynamics of spontaneous MEG activity in brain networks scales *Proc. Natl Acad. Sci. USA* **107** 6040–5

[64] Bartlett M S 1978 *An Introduction to Stochastic Processes with Special Reference to Methods and Applications* 3rd edn (Cambridge: Cambridge University Press)